The Meteoritical Society

Meteoritics & Planetary Science 45, Nr 1, 135–156 (2010)
doi:10.1111/j.1945-5100.2009.01012.x

Analysis of ordinary chondrites using powder X-ray diffraction: 2. Applications to ordinary chondrite parent-body processes

Tasha L. DUNN[1#*], Harry Y. McSWEEN Jr.[1], Timothy J. McCOY[2], and Gordon CRESSEY[3]

[1]Department of Earth and Planetary Sciences, Planetary Geosciences Institute, University of Tennessee, Knoxville, Tennessee 37920, USA
[2]Department of Mineral Sciences, National Museum of Natural History, Smithsonian Institution, Washington, D.C. 20013, USA
[3]Department of Mineralogy, The Natural History Museum, London SW7 5BD, UK
[#]Present address: Tasha L. Dunn, Department of Geography-Geology, Illinois State University, Normal, Illinois 61761, USA
*Corresponding author. E-mail: tldunn@ilstu.edu

(Received 28 May 2008; revision accepted 1 September 2009)

Abstract–We evaluate the chemical and physical conditions of metamorphism in ordinary chondrite parent bodies using X-ray diffraction (XRD)-measured modal mineral abundances and geochemical analyses of 48 type 4–6 ordinary chondrites. Several observations indicate that oxidation may have occurred during progressive metamorphism of equilibrated chondrites, including systematic changes with petrologic type in XRD-derived olivine and low-Ca pyroxene abundances, increasing ratios of MgO/(MgO + FeO) in olivine and pyroxene, mean Ni/Fe and Co/Fe ratios in bulk metal with increasing metamorphic grade, and linear Fe addition trends in molar Fe/Mn and Fe/Mg plots. An aqueous fluid, likely incorporated as hydrous silicates and distributed homogeneously throughout the parent body, was responsible for oxidation. Based on mass balance calculations, a minimum of 0.3–0.4 wt% H_2O reacted with metal to produce oxidized Fe. Prior to oxidation the parent body underwent a period of reduction, as evidenced by the unequilibrated chondrites. Unlike olivine and pyroxene, average plagioclase abundances do not show any systematic changes with increasing petrologic type. Based on this observation and a comparison of modal and normative plagioclase abundances, we suggest that plagioclase completely crystallized from glass by type 4 temperature conditions in the H and L chondrites and by type 5 in the LL chondrites. Because the validity of using the plagioclase thermometer to determine peak temperatures rests on the assumption that plagioclase continued to crystallize through type 6 conditions, we suggest that temperatures calculated using pyroxene goethermometry provide more accurate estimates of the peak temperatures reached in ordinary chondrite parent bodies.

INTRODUCTION

The ordinary chondrites consist of three groups (H, L, and LL) that are distinguished based on variations in bulk composition, such as molecular ratios (FeO/FeO + MgO) in olivine and pyroxene (Mason 1963; Keil and Fredriksson 1964) and the ratio of metallic Fe to total Fe (Dodd et al. 1967). Textural variations and corresponding mineral and chemical trends indicate that differing degrees of thermal metamorphism took place within each chondrite group. Based on these variations, Van Schmus and Wood (1967) developed a petrologic classification scheme for ordinary chondrites. Ordinary chondrites that are relatively unmetamorphosed, or have experienced very slight heating, are designated as type 3 (unequilibrated), whereas chondrites that have undergone the highest degrees of thermal metamorphism are designated as type 6 (equilibrated) (Van Schmus and Wood 1967; McSween et al. 1988). Although the degree of metamorphism varies within each chondrite group, many details regarding the geochemical and thermal changes that take place during this process are not well

understood. Our understanding of parent-body processes has been hampered by an inability to determine precise abundances of the minerals that comprise them.

Using powder X-ray diffraction (XRD), we have quantified the modal abundances of 18 H, 17 L, and 13 LL ordinary chondrites, which together represent the complete petrologic range of equilibrated ordinary chondrites (types 4–6). Because the only ordinary chondrite modal abundances available prior to this study were calculated from Cross, Iddings, Pirsson, Washington (CIPW) norms (McSween et al. 1991), this study represents the first statistically significant sampling of measured modal abundances. In a companion paper, "Analysis of ordinary chondrites using powder X-ray diffraction: 1. Modal mineral abundances" (this issue), we introduce the XRD technique, report the modal abundances of all 48 equilibrated ordinary chondrite samples, and compare our results to modal and normative ordinary chondrite abundances determined in previous studies (e.g., McSween et al. 1991; Gastineau-Lyons et al. 2002). In this paper, we use our XRD-measured modal abundances, along with supplemental chemical analyses, to address two long-standing questions that have hindered our understanding of thermal metamorphism in the parent bodies of ordinary chondrites:

1. Does oxidation or reduction occur in equilibrated ordinary chondrites during progressive metamorphism?
2. What is the best geothermometer to constrain peak metamorphic temperatures in type 6 H, L, and LL ordinary chondrites?

Both of these questions must be resolved in order to develop quantitative thermal evolution models of ordinary chondrite parent asteroids. Redox state has important implications for understanding metamorphic conditions and fluid-rock interactions, and peak metamorphic temperatures (along with cooling rates and duration of heating) are critical input parameters in thermal calculations (McSween et al. 2002).

Oxidation State

Along with bulk iron content, the oxidation state of iron also varies systematically between ordinary chondrite groups, decreasing from LL to L to H. Intragroup variations in mean olivine Fa and low-Ca pyroxene Fs contents (McSween and Labotka 1993), modal abundances of olivine and low-Ca pyroxene (Afiattalab and Wasson 1980; McSween and Labotka 1993), and average Co and Ni concentrations in kamacite (Rubin 1990) also suggest that oxidation state changes within each chondrite group. McSween and Labotka (1993) linked these intragroup redox variations to metamorphic grade and suggested that the equilibrated ordinary chondrites become progressively oxidized during metamorphism by small amounts of aqueous fluid. They proposed the following reaction caused oxidation:

$$\mathrm{Fe(metal)} + \frac{1}{2}\mathrm{O_2} + \mathrm{(Mg,Fe)SiO_3(Px)} = \mathrm{(Mg,\ Fe)_2SiO_4(Ol)}$$

The suggestion that equilibrated ordinary chondrites were oxidized was contrary to existing views that ordinary chondrites were reduced by carbon, either as graphite or CO gas, during metamorphism (e.g., Brett and Sato 1984; Sears and Weeks 1986). Though there is evidence for reduction in ordinary chondrites, this evidence is limited to the unequilibrated (type 3.1–3.9) chondrites. McSween and Labotka (1993) suggested that reduction may have occurred in the unequilibrated chondrites prior to oxidation. This hypothesis was later endorsed by Menzies et al. (2005), who investigated redox state in 21 unequilibrated ordinary chondrites and identified several trends indicative of reduction. The idea that unequilibrated chondrites are reduced does not apply to all samples, however. The presence of carbide-magnetite assemblages, which form under oxidizing conditions, suggests that oxidation took place in at least a few type 3 chondrites, such as Semarkona (Krot et al. 1997).

Because olivine forms at the expense of pyroxene in oxidation reactions proposed by McSween and Labotka (1993), the relative proportions of olivine and low-Ca pyroxene should change with increasing petrologic type if oxidation is occurring. Increasing olivine and decreasing low-Ca pyroxene abundances with petrologic type have been observed in CIPW norms of type 4–6 chondrites (McSween et al. 1991), electron microprobe-measured modal abundances of seven L and LL chondrites (Gastineau-Lyons et al. 2002), and XRD-measured modal abundances of three equilibrated chondrites (Menzies et al. 2005). However, because CIPW normative abundances are not well suited for ordinary chondrites (Dunn et al. 2009) and measured modal data (Gastineau-Lyons et al. 2002; Menzies et al. 2005) are limited, it has been difficult to effectively test the oxidation hypothesis until now.

Peak Temperatures

Peak metamorphic temperatures reached within the interiors of ordinary chondrite parent bodies, along with cooling rates, are critical input parameters in asteroid thermal evolution models (McSween et al. 2002). Peak temperatures are determined by applying

geothermometers to those chondrites that have experienced the highest degree of metamorphism (petrologic type 6). Because several different geothermometers have been used to determine peak temperatures, current estimates for type 6 chondrites range over several hundred degrees. The most common geothermometer used for chondrites is a two-pyroxene geothermometer, based on Ca partitioning between low-Ca and high-Ca pyroxene (Kretz 1982; Lindsley 1983). Several calibrations of this thermometer have been applied to peak temperature estimates in ordinary chondrites (e.g., Olsen and Bunch 1984; McSween and Patchen 1989; Jones 1997; Slater-Reynolds and McSween 2005). However, because results differ depending on the calibration model used or the meteorite examined, estimates for peak metamorphic temperatures vary considerably. The interpretation of pyroxene thermometry is also complicated by the apparent disequilibrium between coexisting low-Ca and high-Ca pyroxenes (McSween and Patchen 1989; Jones 1997; Gastineau-Lyons et al. 2002). Olivine-spinel goethermometry has also been used to estimate peak temperatures in ordinary chondrites (Kessel et al. 2007). However, estimated temperatures are low due to Fe-Mg exchange between olivine and spinel, which continues during cooling.

Alternatively, Nakamuta and Motomura (1999) applied a plagioclase geothermometer (based on Si-Al ordering) to type 6 ordinary chondrites. Nakamuta and Motomura (1999) found that feldspar grains in each chondrite recorded a range of temperatures and assumed that the highest temperature represented peak thermal conditions (~700 °C for H6, 750 °C for L6, and 725 °C for LL6). Peak temperatures estimated using the plagioclase geothermometer, however, are only valid if plagioclase continued to crystallize from chondrule glass through type 6 conditions. Petrologic observations used to develop the Van Schmus and Wood (1967) classification system suggest that all chondrule glass has crystallized to plagioclase by type 5 conditions. Based on modal and normative abundances of plagioclase, Gastineau-Lyons et al. (2002) suggested that plagioclase crystallization was complete at type 5 in LL chondrites and at type 6 in L chondrites.

ANALYTICAL METHODS

Sample Selection

A total of 48 equilibrated ordinary chondrite samples representing each of the ordinary chondrite groups (H, L, and LL) and corresponding petrologic categories 4–6 (Van Schmus and Wood 1967) were selected for modal analysis (Table 1). Unequilibrated (type 3) chondrites are not included in this study, as the question of their redox state (using XRD-derived modal abundances) has been addressed by Menzies et al. (2005). All samples are unbrecciated falls with minimal

Table 1. Chondrites analyzed in this study using X-ray diffraction.

Sample	Class
Benares (a)[a]	LL4
Greenwell Springs	LL4
Hamlet[a]	LL4
Witsand Farm	LL4
Aldsworth[a]	LL5
Alat'ameem	LL5
Olivenza[a]	LL5
Paragould[a]	LL5
Tuxtuac[a]	LL5
Bandong[a]	LL6
Cherokee Spring[a]	LL6
Karatu[a]	LL6
Saint-Severin[a]	LL6
Atarra[a]	L4
Bald Mountain[a]	L4
Rio Negro[a]	L4
Rupota[a]	L4
Ausson[a]	L5
Blackwell	L5
Cilimus	L5
Guibga[a]	L5
Mabwe-Khoywa	L5
Malakal[a]	L5
Messina[a]	L5
Apt[a]	L6
Aumale[a]	L6
Karkh[a]	L6
Kunashak[a]	L6
Kyushu[a]	L6
New Concord[a]	L6
Farmville[a]	H4
Forest Vale	H4
Kabo[a]	H4
Marilia[a]	H4
São Jose do Rio Preto[a]	H4
Allegan[a]	H5
Ehole[a]	H5
Itapicuru-Mirim	H5
Lost City[a]	H5
Príbram[a]	H5
Schenectady[a]	H5
Uberaba	H5
Andura[a]	H6
Butsura[a]	H6
Canon City[a]	H6
Chiang Khan	H6
Guareña[a]	H6
Ipiranga[a]	H6

[a]Denotes sample in which olivine and low-Ca pyroxene were analyzed using electron microprobe.

weathering and low shock. Thirty-seven of these samples were originally prepared for bulk chemical analysis by E. Jarosewich as part of the Smithsonian Institution's Analyzed Meteorite Powder Collection. Small chips of the remaining 11 chondrites were acquired from the Natural History Museum (NHM) and from the Smithsonian Institution (SI). These samples were crushed to a powder consistency and prepared for analysis at the University of Tennessee and the NHM. (We refer the reader to Dunn et al. [2009] for a detailed description of XRD sample preparation.) Polished thin sections of 38 of these ordinary chondrites were acquired from the NHM and from the SI so that compositions of olivine and low-Ca pyroxene could be determined.

X-Ray Diffraction

XRD data were collected using an INEL curved position-sensitive detector (PSD) (INEL, Arteny, France) at the NHM in London, England. The INEL PSD has an output of 4096 channels (each 0.03° 2θ wide), which represents a total arc of 120° 2θ. Using a fixed detector, diffracted intensity is simultaneously measured at all angles, resulting in rapid collection of diffraction patterns. The precision of diffraction patterns is improved by the use of an anode blade rather than a traditional anode wire. Experimental configurations in this study are similar to those implemented by Bland et al. (2004) and Menzies et al. (2005). Samples were radiated using CuKα1 radiation, which was selected from the primary beam using a single-crystal Ge111 monochromator. Post-monochromator slits were used to restrict the beam size to 0.24 × 3.0 mm. Diffraction patterns were recorded in reflection geometry from the top of the sample smear, which was set at an angle 7.5° to the incident beam.

The PSD-XRD method for quantification of multi-phase samples (hereafter referred to as powder XRD) was first introduced by Cressey and Schofield (1996) and further developed by Batchelder and Cressey (1998). Modal abundances are determined by fitting peak intensities of a mineral standard to those present in a mixture. The intensity of the whole pattern standard phase is decreased by a factor to match the intensity of that phase in the mixture and then subtracted, effectively removing that component from the mixture pattern. This procedure is repeated until all phases have been removed. After applying a simple correction for deadtime of the detector, the actual weight percent of each mineral is determined using the pattern-fit fraction of a single phase and the calculated mass absorption coefficients for each mineral in the mixture (Batchelder and Cressey 1998). Weight percentages can be converted to volume percents if the density of each mineral phase is known. However, in this study all results are presented in weight percent to allow for ease of comparison with previously determined normative abundances (McSween et al. 1991). For a detailed description of this powder XRD technique and its application to ordinary chondrite modal abundances, see Dunn et al. (2009).

Electron Microprobe Phase Analysis

Olivine, low-Ca pyroxene, and high-Ca pyroxene compositions were determined with a Cameca SX-50 electron microprobe at the University of Tennessee, using synthetic and natural mineral standards. Data were corrected using ZAF (PAP) procedures. Standard operating conditions during analysis included 15 kV potential, 20–30 nA beam current, and a 2 μm beam size. Counting time was typically 20 s. Olivine and low-Ca pyroxene grains were chosen randomly for analysis by moving the sample stage in a grid pattern and analyzing grains in the backscatter image field of view, resulting in a representative sampling of the entire sample. Grains larger than 30 μm were selected to ensure quality analyses, and 15–20 grains of both olivine and low-Ca pyroxene were analyzed per thin section. Unlike low-Ca pyroxene, which comprises one-third to one-fourth of ordinary chondrite modes, high-Ca pyroxene is present at very low abundances and can be difficult to recognize and analyze. High-Ca pyroxene was identified in nine type 6 chondrites, and one to eight analyses were collected per sample. High-Ca pyroxene was analyzed in type 6 chondrites only for the purpose of calculating peak metamorphic temperatures.

EVALUATION OF REDOX STATE IN EQUILIBRATED CHONDRITES

Olivine and Low-Ca Pyroxene Modal Abundances

Modal abundances of olivine and low-Ca pyroxene show subtle but systematic variations with petrologic type in all chondrite groups (H, L, and LL). Average abundances and standard deviations of olivine and low-Ca pyroxene are listed in Table 2. Figure 1 illustrates changes in mean olivine and low-Ca pyroxene abundances (with petrologic type) in the H, L, and LL chondrites. In all three chondrite groups, average olivine abundances increase with increasing metamorphic grade. In the H and LL chondrites, the converse trend is present in low-Ca pyroxene abundances. However, this trend of decreasing low-Ca pyroxene abundances is slightly askew in the L chondrites, as average low-Ca pyroxene abundances show an overall decrease from type 4 to type 6, but increase between type 4 and type 5. The average abundance of low-Ca pyroxene in the L5

Table 2. Average abundances of olivine, low-Ca pyroxene, and plagioclase.

Chondrite group	Number of analyses	Olivine	Low-Ca pyroxene	Plagioclase
H4	5	29.8 (0.4)	27.0 (1.1)	9.1 (0.5)
H5	7	33.1 (2.0)	25.2 (1.1)	8.9 (0.7)
H6	6	35.7 (2.2)	24.9 (2.1)	8.9 (0.4)
L4	4	40.7 (1.9)	23.6 (1.8)	9.5 (0.4)
L5	7	42.2 (2.0)	24.1 (1.3)	9.3 (1.5)
L6	6	43.0 (1.6)	21.7 (0.9)	9.5 (0.5)
LL4	4	49.7 (1.4)	22.6 (1.4)	9.7 (1.2)
LL5	5	51.1 (1.1)	21.8 (1.3)	9.6 (0.6)
LL6	4	52.5 (3.1)	18.9 (1.0)	9.9 (0.7)

Values are in wt%. 1σ standard deviations are shown in parentheses.

chondrites is higher than that of the L6 chondrites due to individual low-Ca pyroxene abundances in Ausson, Blackwell, and Cilimus, which are 1–2 wt% higher than other L5 chondrites. It is possible that these abundances are inaccurate due to unrepresentative sampling. Powders of Ausson, Blackwell, and Cilimus were prepared from small chip weighing 0.1–0.5 g, which may not be enough material to provide representative modal mineralogies. For a detailed discussion of representative sampling in this study, refer to Dunn et al. (2009).

The trends present in mean abundances of olivine and low-Ca pyroxene are subtle and may seem unconvincing. Most changes in modal abundances between petrologic types are within the error of the powder XRD technique, as measured by Dunn et al. (2009) (±2.2 wt%), and trends are indistinct when 1σ standard deviations are considered. However, these trends become more obvious if we consider instead the overall change in abundance with metamorphism (i.e., from petrologic type 4 to type 6). In the H chondrites olivine abundances increase from type 4 to type 6 by 5.9 wt%, in the Ls by 2.3 wt%, and in the LLs by 2.8 wt%. Conversely, low-Ca pyroxene abundances decrease by 2.1 wt% in the H chondrites, 1.9 wt% in the Ls, and 3.7 wt% in the LLs. Standard deviation is still a problem when discerning overall trends, but there is an apparent increase in olivine in the H chondrites and a decrease in low-Ca pyroxene in the LL chondrites. In addition, an ANOVA single factor test indicates that the differences between overall abundances are statistically significant in the H chondrites (in olivine) in the L and LL chondrites (in low-Ca pyroxene) at 95% confidence levels.

The relationship between average olivine and low-Ca pyroxene abundances can be expressed simply as a ratio of Ol/Opx. Ratios of olivine to low-Ca pyroxene (Ol/Px) in ordinary chondrites have been calculated from normative abundances (McSween et al. 1991),

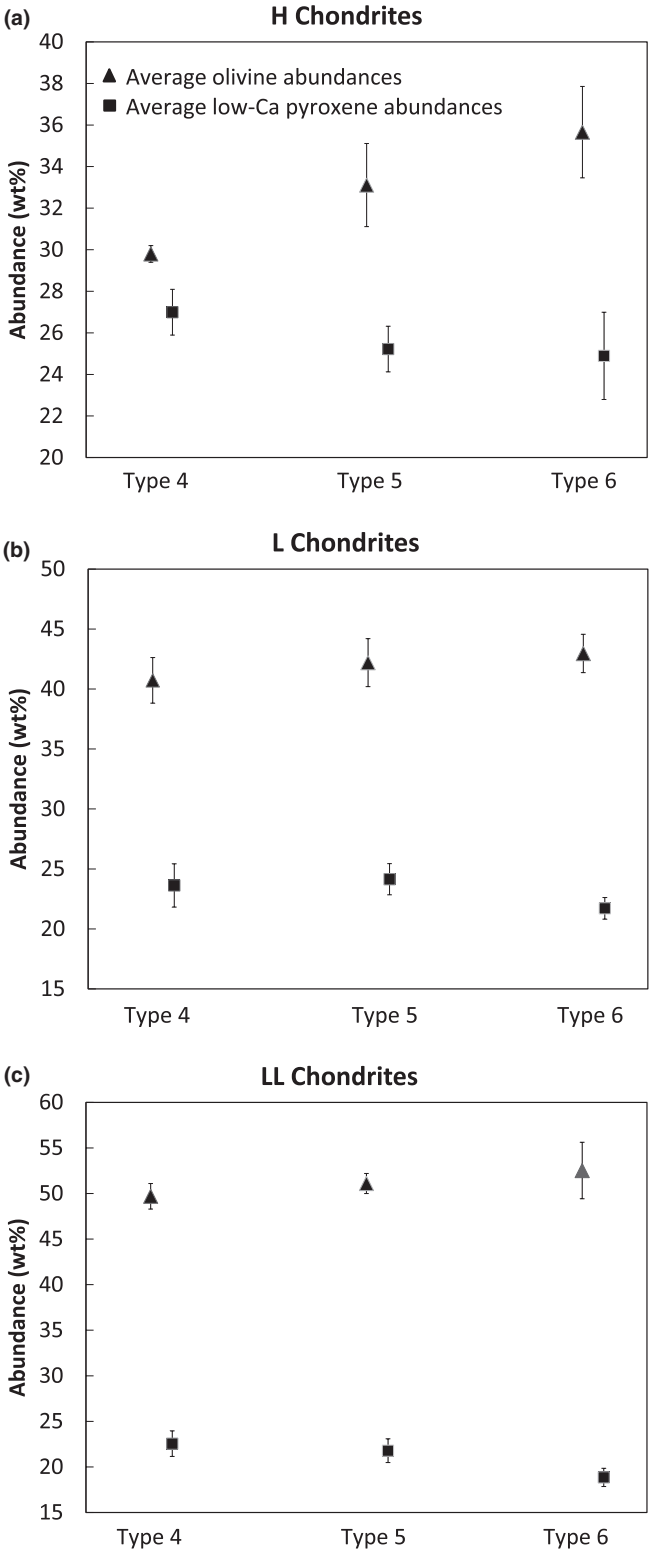

Fig. 1. Average XRD-measured olivine and low-Ca pyroxene abundances for each petrologic type. Error bars are 1σ standard deviations of mean abundances. Average abundances and standard deviations are listed in Table 2.

modal abundances (Gastineau-Lyons et al. 2002), and VIS/NIR reflectance spectra (Gastineau-Lyons et al. 2002; Burbine et al. 2003). XRD-measured modal Ol/Opx ratios for the chondrites in this study are shown in Fig. 2, along with ratios calculated from normative data (McSween et al. 1991). As indicated in paper 1, normative olivine abundances are consistently higher than XRD-derived abundances due to incorrect allocation of oxides in the normative calculation. As a result, normative ratios of Ol/Opx are higher than measured ratios. Despite the difference between olivine abundances, both modal and normative Ol/Opx ratios increase with increasing petrologic type in the H, L, and LL chondrites. We suggest that the presence of this trend in both data sets is significant. Despite the flaws in normative calculations, the proportions of olivine and low-Ca pyroxene in normative abundances appear to support the hypothesis that progressive oxidation is occurring between petrologic type 4 and type 6.

It is worth noting that the trends represented by changes in Ol/Opx ratios are not linear, which appear to indicate that temperature intervals are not constant between each petrologic type. This is not unexpected though, as temperature ranges, calculated using thermometry, often overlap between petrologic types. In the LL chondrites, equilibration temperatures calculated using the olivine-spinel thermometer range from 648 to 670 °C in type 4, 677–741 °C in type 5, and 683–777 °C in type 6 (Kessel et al. 2007). Although these calculated temperatures are lower than expected due to continued Fe-Mg exchange after cooling, the Kessel et al. (2007) study presents an extensive survey of samples and should not be ignored. We must consider these temperature variations when interpreting mineralogical and chemical data, as peak temperatures and duration of metamorphism vary among samples within a petrologic type. Each sample is, in essence, a product of the effects of metamorphism throughout its entire thermal history.

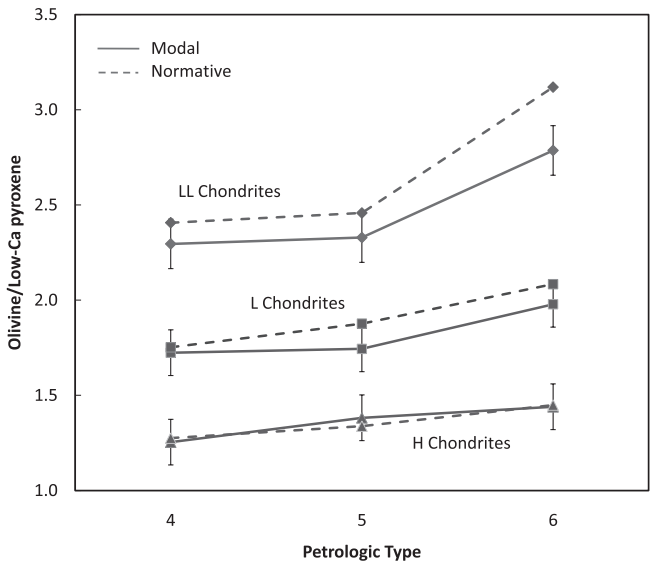

Fig. 2. Ol/Px ratios of H, L, and LL chondrites determined from modal data (this study) and normative data (McSween et al. 1991). Ratios in both sets of data increase from petrologic type 4 to petrologic type 6.

Although the high standard deviation makes it difficult to state with absolute certainty that oxidation is increasing with increasing petrologic type, it may allow for a more useful observation; it may indicate that the oxidation state varies slightly within each petrologic type. In other words, not all type 4 chondrites may have experienced the same degree of oxidation. The same is true for type 5 and type 6. Previous studies could not have recognized this variability due to their limited sample populations. For example, in Gastineau-Lyons et al. (2002) only one sample of each petrologic type was examined. This observation appears to indicate that the redox state in the ordinary chondrites is a complex process driven by several factors, including the amount of oxidizing agent available, the temperature within the parent body, and the kinetics of the oxidizing reaction.

Olivine and Low-Ca Pyroxene Mineral Chemistry

Of the 48 equilibrated ordinary chondrites examined in this study, 38 were analyzed using the electron microprobe to determine olivine and low-Ca pyroxene compositions. Average olivine analyses of H, L, and LL chondrites are reported in Tables 3–5 and low-Ca pyroxene in Tables 6–8. In this section, we examine compositional data of silicate minerals to look for chemical trends indicative of oxidation. As bulk geochemical analyses from previous studies (Kallemeyn et al. 1989) indicate that there are no systematic compositional differences among ordinary chondrites of differing petrologic types, we base our interpretations in this section on the fundamental assumptions that thermal metamorphism was isochemical and that chondrites from each group were derived from a common, unequilibrated starting material.

Intragroup variations in the molecular ratios of olivine (mol% Fa) and low-Ca pyroxene (mol% Fs) have been recognized in several previous studies (Scott et al. 1986; Rubin 1990; McSween and Labotka 1993) and have been attributed to progressive oxidation with increasing thermal metamorphism (Rubin 1990). Olivine (mol% Fa) and low-Ca pyroxene (mol% Fs) compositions of each ordinary chondrite analyzed in this study are presented in Fig. 3. Mean compositions of olivine and low-Ca

Table 3. Average electron microprobe analyses for olivine in each H chondrite.

	Farmville H4 [16]	Kabo H4 [13]	São Jose do Rio Preto H4 [16]	Allegan H5 [14]	Ehole H5 [17]	Itapicura Mirim H5 [14]	Lost City H5 [20]	Príbram H5 [14]	Schnectady H5 [21]	Andura H6 [17]	Butsura H6 [17]	Canon City H6 [18]	Guareña H6 [13]	Ipiranga H6 [16]
SiO_2	39.1 (4)	39.1 (3)	38.8 (6)	39.1 (5)	38.5 (3)	39.0 (4)	39.0 (2)	38.6 (4)	38.5 (6)	39.6 (4)	39.6 (4)	39.9 (3)	40.0 (4)	39.8 (3)
Cr_2O_3	< 0.03	< 0.03	0.03 (8)	0.03 (3)	0.03 (3)	0.03 (4)	< 0.03	0.08 (23)	0.04 (10)	< 0.03	0.09 (35)	0.02 (3)	< 0.03	< 0.03
FeO	16.5 (3)	17.1 (4)	17.6 (3)	16.7 (4)	18.0 (3)	17.4 (3)	17.6 (2)	17.4 (3)	17.7 (6)	18.0 (3)	17.7 (3)	17.8 (2)	18.1 (2)	17.7 (3)
MnO	0.45 (4)	0.47 (3)	0.50 (3)	0.48 (3)	0.46 (3)	0.47 (3)	0.47 (3)	0.46 (3)	0.45 (3)	0.47 (3)	0.45 (4)	0.46 (4)	0.47 (5)	0.46 (3)
MgO	43.5 (3)	43.0 (4)	42.5 (4)	43.3 (4)	42.1 (4)	43.4 (3)	43.0 (3)	43.0 (3)	42.5 (2)	42.2 (3)	42.1 (3)	42.1 (2)	42.7 (2)	43.0 (3)
CaO	0.03 (1)	< 0.03	0.04 (4)	0.08 (14)	< 0.03	< 0.03	0.03 (1)	< 0.03	< 0.03	0.03 (1)	0.04 (1)	0.03 (7)	< 0.03	< 0.03
Total	99.6	99.6	99.5	99.7	99.1	100.2	100.1	99.6	99.2	100.3	100.0	100.3	101.3	101.0
Cations based on 4 oxygens														
Si	0.99	1.00	0.99	1.00	0.99	0.99	0.99	0.99	0.99	1.00	1.01	1.01	1.00	1.00
Cr	0.00	0.00	0.00	0.00	0.00	0.00	0.00	0.00	0.00	0.00	0.00	0.00	0.00	0.00
Fe	0.35	0.36	0.38	0.35	0.39	0.37	0.37	0.37	0.38	0.38	0.38	0.38	0.38	0.37
Mn	0.01	0.01	0.01	0.01	0.01	0.01	0.01	0.01	0.01	0.01	0.01	0.01	0.01	0.01
Mg	1.65	1.63	1.63	1.64	1.62	1.64	1.63	1.64	1.63	1.60	1.60	1.59	1.60	1.61
Ca	0.00	0.00	0.00	0.00	0.00	0.00	0.00	0.00	0.00	0.00	0.00	0.00	0.00	0.00
Total	3.01	3.00	3.01	3.00	3.01	3.01	3.01	3.01	3.01	3.00	2.99	2.99	3.00	3.00
Fe/Mn	35.9	36.3	37.3	34.6	38.2	36.3	36.9	36.7	39.5	37.9	38.9	38.7	38.1	37.6
Fe/Mg	0.21	0.22	0.23	0.22	0.24	0.22	0.23	0.23	0.23	0.24	0.24	0.24	0.24	0.23
Fa	17.6	18.2	18.9	17.7	19.3	18.3	18.7	18.5	19.0	19.3	19.1	19.2	19.2	18.7

Numbers in square brackets represent number of analyses averaged.
Numbers in parentheses represent 1σ precision of replicate analyses expressed as the least digit cited.

Table 4. Average electron microprobe analyses for olivine in each L chondrite.

	Atarra L4 [19]	Bald Mountain L4 [20]	Rio Negro L4 [20]	Rupota L4 [20]	Guibga L5 [21]	Ausson L5 [20]	Malakal L5 [12]	Messina L5 [14]	Apt L6 [15]	Aumale L6 [12]	Karkh L6 [10]	Kunashak L6 [17]	Kyushu L6 [17]	New Concord L6 [15]
SiO_2	38.2 (4)	38.2 (4)	38.3 (4)	38.1 (2)	38.3 (2)	37.9 (2)	37.2 (5)	37.9 (5)	37.9 (3)	37.9 (3)	37.8 (6)	38.3 (4)	37.9 (4)	37.7 (3)
Cr_2O_3	0.11 (38)	0.09 (23)	0.03 (3)	< 0.03	0.04 (11)	< 0.03	0.04 (5)	< 0.03	< 0.03	< 0.03	< 0.03	0.03 (2)	< 0.03	0.03 (12)
FeO	21.4 (3)	21.3 (3)	22.5 (15)	22.4 (4)	22.1 (4)	22.7 (2)	22.8 (7)	22.6 (4)	22.9 (4)	22.4 (3)	22.7 (6)	22.8 (4)	22.4 (3)	22.2 (4)
MnO	0.46 (3)	0.46 (4)	0.46 (4)	0.46 (4)	0.45 (4)	0.49 (3)	0.48 (4)	0.48 (3)	0.44 (4)	0.46 (3)	0.45 (3)	0.47 (4)	0.47 (4)	0.49 (24)
MgO	39.7 (4)	40.1 (4)	38.9 (11)	38.8 (3)	39.2 (4)	38.8 (2)	38.8 (6)	39.0 (4)	38.4 (4)	38.9 (3)	38.6 (6)	39.2 (4)	38.8 (2)	38.6 (3)
CaO	0.03 (2)	< 0.03	0.04 (3)	0.05 (2)	< 0.03	< 0.03	< 0.03	0.04 (2)	0.03 (1)	< 0.03	0.04 (1)	0.12 (21)	0.03 (1)	0.06 (3)
Total	99.9	100.1	100.3	99.9	100.2	100.0	99.3	100.0	99.8	99.7	99.7	100.9	99.6	99.0
Cations based on 4 oxygens														
Si	0.99	0.99	1.00	1.00	1.00	0.99	0.98	0.99	0.99	0.99	0.99	0.99	0.99	0.99
Cr	0.00	0.00	0.00	0.00	0.00	0.00	0.00	0.00	0.00	0.00	0.00	0.00	0.00	0.00
Fe	0.46	0.46	0.49	0.49	0.48	0.50	0.50	0.49	0.50	0.49	0.50	0.49	0.49	0.49
Mn	0.01	0.01	0.01	0.01	0.01	0.01	0.01	0.01	0.01	0.01	0.01	0.01	0.01	0.01
Mg	1.54	1.55	1.51	1.51	1.52	1.51	1.52	1.52	1.50	1.52	1.51	1.51	1.51	1.52
Ca	0.00	0.00	0.00	0.00	0.00	0.00	0.00	0.00	0.00	0.00	0.00	0.00	0.00	0.00
Total	3.01	3.01	3.00	3.00	3.00	3.01	3.02	3.01	3.01	3.01	3.01	3.01	3.01	3.01
Fe/Mn	46.2	46.2	46.2	48.9	48.5	46.2	47.9	46.0	51.2	48.9	50.5	48.5	47.2	46.7
Fe/Mg	0.30	0.30	0.30	0.32	0.32	0.33	0.33	0.33	0.33	0.32	0.33	0.33	0.32	0.32
Fa	23.2	22.9	24.5	24.5	24.1	24.7	24.8	24.5	25.1	24.5	24.8	24.6	24.5	24.3

Numbers in square brackets represent number of analyses averaged.
Numbers in parentheses represent 1σ precision of replicate analyses expressed as the least digit cited.

Table 5. Average electron microprobe analyses for olivine in each LL chondrite.

	Bernares (a) LL4 [16]	Hamlet LL4 [12]	Aldsworth LL5 [20]	Olivenza LL5 [19]	Paragould LL5 [17]	Tuxtuac LL5 [17]	Bandong LL6 [17]	Cherokee Springs LL6 [17]	Karatu LL6 [19]	Saint-Severin LL6 [19]
SiO_2	37.3 (3)	37.4 (4)	37.2 (5)	37.2 (2)	37.8 (3)	36.9 (3)	37.2 (3)	37.6 (3)	37.1 (5)	37.4 (4)
Cr_2O_3	0.07 (18)	< 0.03	0.17 (52)	< 0.03	0.08 (9)	< 0.03	0.03 (2)	0.04 (12)	0.03 (8)	0.01 (2)
FeO	26.0 (2)	25.3 (16)	25.4 (3)	27.1 (3)	25.2 (4)	27.1 (3)	27.6 (5)	25.8 (3)	28.1 (5)	27.0 (5)
MnO	0.51 (5)	0.46 (3)	0.47 (5)	0.44 (3)	0.46 (5)	0.44 (5)	0.44 (6)	0.45 (3)	0.45 (5)	0.45 (5)
MgO	35.9 (2)	38.6 (13)	36.3 (3)	35.4 (2)	36.8 (4)	34.9 (3)	35.3 (6)	36.7 (3)	34.9 (5)	35.8 (3)
CaO	0.05 (2)	0.04 (2)	0.04 (3)	0.04 (1)	0.08 (3)	0.05 (5)	0.05 (2)	0.04 (1)	0.04 (3)	0.06 (2)
Total	99.8	100.1	99.7	100.1	100.4	99.5	100.7	100.7	100.6	100.6
Cations based on 4 oxygens										
Si	0.99	0.990	0.99	0.99	0.99	0.99	0.99	0.99	0.99	0.99
Cr	0.00	0.00	0.00	0.00	0.00	0.00	0.00	0.00	0.00	0.00
Fe	0.58	0.56	0.57	0.60	0.55	0.61	0.61	0.57	0.63	0.60
Mn	0.01	0.01	0.01	0.01	0.01	0.01	0.01	0.01	0.01	0.01
Mg	1.42	1.45	1.44	1.41	1.44	1.40	1.40	1.44	1.39	1.41
Ca	0.00	0.00	0.00	0.00	0.00	0.00	0.00	0.00	0.00	0.00
Total	3.01	3.01	3.01	3.01	3.01	3.01	3.01	3.01	3.01	3.01
Fe/Mn	50.0	53.7	53.9	60.9	54.1	60.9	63.2	55.3	62.6	59.9
Fe/Mg	0.41	0.39	0.39	0.43	0.38	0.44	0.44	0.40	0.45	0.42
Fa	28.9	26.5	28.2	30.0	27.7	30.4	30.5	28.3	31.1	29.7

Numbers in square brackets represent number of analyses averaged.
Numbers in parentheses represent 1σ precision of replicate analyses expressed as the least digit cited.

Table 6. Average electron microprobe analyses for low-Ca pyroxene in each H chondrite.

	Farmville H4 [12]	Kabo H4 [18]	São Jose do Rio Preto H4 [16]	Allegan H5 [14]	Ehole H5 [16]	Itapicura Mirim H5 [14]	Lost City H5 [19]	Príbram H5 [14]	Schnectady H5 [12]	Andura H6 [13]	Butsura H6 [13]	Canon City H6 [12]	Guareña H6 [9]	Ipiranga H6 [13]
SiO_2	55.9 (6)	55.9 (5)	55.7 (7)	56.3 (8)	55.3 (6)	56.1 (7)	56.1 (3)	55.8 (7)	55.4 (6)	57.1 (5)	56.8 (8)	57.1 (5)	57.6 (4)	57.0 (6)
TiO_2	0.18 (9)	0.11 (8)	0.14 (7)	0.22 (11)	0.17 (8)	0.17 (5)	0.16 (7)	0.17 (5)	0.13 (5)	0.18 (4)	0.19 (6)	0.18 (5)	0.17 (4)	0.20 (6)
Al_2O_3	0.36 (29)	0.33 (37)	0.23 (20)	0.25 (19)	0.15 (10)	0.35 (45)	0.20 (11)	0.21 (9)	0.22 (22)	0.25 (26)	0.20 (6)	0.21 (12)	0.16 (7)	0.20 (7)
Cr_2O_3	0.40 (61)	0.20 (15)	0.39 (53)	0.24 (21)	0.13 (18)	0.29 (33)	0.19 (12)	0.12 (2)	0.11 (4)	0.12 (3)	0.15 (8)	0.15 (6)	0.11 (2)	0.13 (5)
FeO	10.6 (3)	10.9 (2)	11.1 (3)	10.6 (2)	11.3 (2)	11.1 (4)	11.0 (1)	11.3 (5)	11.3 (2)	11.2 (3)	11.3 (10)	11.2 (1)	11.4 (1)	11.3 (6)
MnO	0.51 (3)	0.48 (4)	0.50 (3)	0.50 (5)	0.50 (6)	0.50 (4)	0.49 (3)	0.49 (4)	0.51 (3)	0.48 (3)	0.47 (3)	0.59 (2)	0.52 (4)	0.50 (4)
MgO	31.3 (4)	30.8 (5)	31.0 (4)	31.3 (3)	30.4 (33)	30.9 (8)	31.2 (2)	31.0 (3)	31.0 (2)	30.8 (2)	30.5 (3)	30.7 (2)	30.9 (2)	31.1 (2)
CaO	0.58 (8)	0.59 (11)	0.59 (8)	0.67 (10)	0.74 (52)	0.81 (10)	0.70 (11)	0.70 (10)	0.67 (7)	0.71 (14)	0.82 (13)	0.80 (5)	0.72 (13)	0.71 (9)
Na_2O	< 0.03	0.06 (13)	< 0.03	< 0.03	< 0.03	0.07 (15)	0.03 (1)	< 0.03	0.05 (10)	< 0.03	< 0.03	< 0.03	< 0.03	< 0.03
Total	99.9	99.4	99.8	100.1	98.7	100.2	100.0	99.8	99.3	100.8	100.5	100.8	101.5	101.1
Cations based on 6 oxygens														
Si	1.98	1.99	1.98	1.98	1.98	1.98	1.98	1.98	1.98	2.00	2.00	2.00	2.00	1.99
Ti	0.00	0.00	0.00	0.01	0.00	0.00	0.00	0.00	0.00	0.00	0.01	0.00	0.00	0.01
Al	0.04	0.01	0.01	0.01	0.01	0.01	0.01	0.01	0.01	0.01	0.01	0.01	0.01	0.01
Cr	0.01	0.01	0.01	0.01	0.00	0.01	0.01	0.00	0.00	0.00	0.00	0.00	0.00	0.00
Fe	0.30	0.32	0.33	0.31	0.34	0.33	0.32	0.34	0.34	0.33	0.33	0.33	0.33	0.33
Mn	0.01	0.01	0.01	0.01	0.02	0.02	0.01	0.01	0.02	0.01	0.01	0.01	0.02	0.01
Mg	1.60	1.63	1.64	1.64	1.63	1.62	1.64	1.64	1.65	1.61	1.60	1.60	1.60	1.62
Ca	0.03	0.02	0.02	0.03	0.03	0.03	0.03	0.03	0.03	0.03	0.03	0.03	0.03	0.03
Na	0.01	0.00	0.00	0.00	0.00	0.00	0.00	0.00	0.00	0.00	0.00	0.00	0.00	0.00
Total	4.00	4.00	4.01	4.00	4.01	4.01	4.01	4.01	4.02	3.99	3.99	3.99	3.99	4.00
Fe/Mn	20.5	22.7	22.3	20.9	22.1	21.7	22.3	22.8	21.9	23.4	23.9	22.2	22.1	22.2
Fe/Mg	0.19	0.20	0.20	0.19	0.21	0.20	0.20	0.20	0.20	0.20	0.21	0.20	0.21	0.20
Fs	16.5	16.9	17.2	16.4	17.0	17.1	16.9	17.4	17.4	17.3	17.5	17.3	17.5	17.3
Wo	1.1	1.1	1.1	1.3	3.8	1.5	1.3	1.3	1.3	1.3	1.6	1.5	1.4	1.3

Numbers in square brackets represent number of analyses averaged.

Numbers in parentheses represent 1σ precision of replicate analyses expressed as the least digit cited.

Table 7. Average electron microprobe analyses for low-Ca pyroxene in each L chondrite.

	Attara L4 [16]	Bald Mountain L4 [17]	Rio Negro L4 [18]	Rupota L4 [18]	Ausson L5 [18]	Guibga L5 [18]	Malakal L5 [12]	Messina L5 [14]	Apt L6 [12]	Aumale L6 [12]	Karkh L6 [13]	Kunashak L6 [20]	Kyushu L6 [13]	New Concord L6 [12]
SiO_2	55.6 (6)	55.5 (4)	55.4 (7)	55.4 (2)	55.0 (6)	55.4 (5)	54.7 (7)	55.1 (10)	54.9 (7)	54.9 (4)	54.7 (7)	55.3 (4)	55.2 (3)	55.0 (4)
TiO_2	0.14 (8)	0.13 (7)	0.15 (6)	0.18 (6)	0.14 (6)	0.17 (4)	0.20 (11)	0.19 (2)	0.18 (2)	0.19 (4)	0.19 (3)	0.21 (5)	0.18 (2)	0.18 (3)
Al_2O_3	0.16 (10)	0.18 (10)	0.36 (62)	0.23 (19)	0.13 (7)	0.17 (8)	0.33 (44)	0.18 (8)	0.19 (12)	0.16 (6)	0.24 (8)	0.24 (9)	0.20 (12)	0.22 (15)
Cr_2O_3	0.15 (10)	0.19 (14)	0.40 (47)	0.21 (16)	0.11 (5)	0.21 (40)	0.17 (18)	0.12 (5)	0.10 (3)	0.11 (10)	0.19 (10)	0.18 (12)	0.11 (4)	0.11 (4)
FeO	13.2 (8)	13.0 (5)	13.4 (7)	13.4 (10)	13.7 (2)	13.7 (3)	13.9 (4)	13.8 (4)	14.3 (7)	13.9 (15)	14.2 (7)	13.8 (6)	13.6 (3)	13.5 (4)
MnO	0.45 (4)	0.49 (4)	0.46 (4)	0.46 (8)	0.48 (3)	0.46 (4)	0.47 (3)	0.48 (6)	0.47 (3)	0.48 (5)	0.49 (3)	0.49 (4)	0.48 (4)	0.48 (2)
MgO	29.9 (5)	29.8 (6)	29.4 (7)	29.0 (7)	29.0 (5)	29.2 (2)	28.8 (6)	29.1 (3)	28.5 (4)	28.9 (20)	28.6 (4)	29.2 (7)	28.9 (2)	28.8 (4)
CaO	0.41 (9)	0.80 (83)	0.7 (40)	1.02 (29)	0.72 (8)	0.64 (15)	0.79 (13)	0.84 (20)	0.77 (12)	0.74 (33)	1.11 (34)	1.04 (11)	0.85 (15)	0.91 (48)
Na_2O	0.03 (2)	< 0.03	0.05 (3)	0.03 (2)	< 0.03	0.03 (1)	0.08 (17)	0.03 (2)	< 0.03	< 0.03	0.04 (3)	0.04 (3)	0.03 (2)	< 0.03
Total	100.0	100.1	100.2	99.9	99.4	100.0	99.4	99.9	99.5	99.4	99.7	100.6	99.6	99.3
Cations based on 6 oxygens														
Si	1.98	1.98	1.98	1.98	1.98	1.98	1.97	1.98	1.98	1.98	1.97	1.97	1.98	1.98
Ti	0.00	0.00	0.00	0.00	0.00	0.00	0.01	0.01	0.00	0.00	0.01	0.01	0.00	0.00
Al	0.01	0.01	0.02	0.01	0.01	0.01	0.01	0.01	0.01	0.01	0.01	0.01	0.01	0.01
Cr	0.00	0.01	0.01	0.01	0.00	0.01	0.00	0.00	0.00	0.00	0.01	0.01	0.00	0.00
Fe	0.39	0.39	0.40	0.40	0.41	0.41	0.42	0.42	0.43	0.42	0.43	0.41	0.41	0.41
Mn	0.01	0.01	0.01	0.01	0.01	0.01	0.01	0.01	0.01	0.01	0.01	0.01	0.01	0.01
Mg	1.59	1.59	1.56	1.55	1.56	1.56	1.55	1.56	1.53	1.55	1.54	1.55	1.55	1.55
Ca	0.02	0.03	0.03	0.04	0.03	0.02	0.03	0.03	0.03	0.03	0.04	0.04	0.03	0.03
Na	0.00	0.00	0.00	0.00	0.00	0.00	0.01	0.00	0.00	0.00	0.00	0.00	0.00	0.00
Total	4.01	4.01	4.01	4.01	4.01	4.01	4.02	4.01	4.01	4.01	4.02	4.02	4.01	4.01
Fe/Mn	28.9	26.3	29.2	29.2	28.0	29.4	29.2	28.4	30.4	28.3	28.8	27.7	27.9	27.9
Fe/Mg	0.25	0.24	0.26	0.26	0.27	0.26	0.27	0.27	0.28	0.27	0.28	0.26	0.26	0.26
Fs	20.2	19.9	20.6	20.7	21.3	21.2	21.5	21.3	22.2	21.0	21.8	21.1	21.1	21.1
Wo	0.8	1.5	1.3	2.0	1.4	1.2	1.5	1.6	1.5	3.2	2.1	2.0	1.6	1.7

Numbers in square brackets represent number of analyses averaged.

Numbers in parentheses represent 1σ precision of replicate analyses expressed as the least digit cited.

Table 8. Average electron microprobe analyses for low-Ca pyroxene in each LL chondrite.

	Benares (a) LL4 [12]	Hamlet LL4 [14]	Aldsworth LL5 [15]	Olivenza LL5 [18]	Paragould LL5 [17]	Tuxtuac LL5 [14]	Bandong LL6 [16]	Cherokee Springs LL6 [19]	Karatu LL6 [17]	Saint-Severin LL6 [19]
SiO_2	54.3 (8)	54.7 (11)	54.6 (3)	54.7 (3)	55.2 (4)	54.5 (3)	54.6 (5)	55.1 (3)	54.5 (4)	54.8 (3)
TiO_2	0.15 (9)	0.09 (9)	0.12 (6)	0.15 (5)	0.14 (7)	0.19 (10)	0.20 (3)	0.19 (5)	0.21 (2)	0.20 (2)
Al_2O_3	0.42 (70)	0.70 (12)	0.30 (24)	0.13 (4)	0.16 (8)	0.17 (12)	0.23 (14)	0.16 (3)	0.22 (12)	0.18 (2)
Cr_2O_3	0.31 (38)	0.46 (32)	0.21 (18)	0.11 (7)	0.17 (6)	0.10 (6)	0.17 (13)	0.10 (3)	0.15 (3)	0.16 (7)
FeO	15.1 (8)	14.5 (22)	15.3 (4)	16.1 (1)	15.4 (4)	16.3 (3)	16.5 (3)	15.4 (2)	17.0 (3)	16.0 (3)
MnO	0.44 (4)	0.44 (9)	0.44 (4)	0.44 (3)	0.45 (3)	0.45 (4)	0.43 (5)	0.46 (3)	0.44 (4)	0.45 (4)
MgO	27.2 (9)	28.0 (20)	27.9 (5)	27.4 (1)	27.9 (5)	27.2 (2)	27.3 (4)	28.1 (2)	26.9 (3)	27.7 (3)
CaO	1.20 (10)	0.98 (93)	0.81 (65)	0.79 (13)	0.87 (33)	0.76 (17)	1.04 (18)	0.87 (12)	1.12 (1)	0.89 (8)
Na_2O	0.08 (5)	0.06 (7)	0.04 (3)	<0.03	<0.03	<0.03	0.03 (1)	0.03 (2)	0.06 (6)	0.03 (2)
Total	99.2	99.9	99.7	99.9	100.3	99.8	100.5	100.5	100.6	100.4
Cations based on 6 oxygens										
Si	1.98	1.97	1.98	1.98	1.98	1.98	1.97	1.98	1.97	1.97
Ti	0.00	0.00	0.00	0.00	0.00	0.01	0.01	0.01	0.01	0.01
Al	0.02	0.03	0.01	0.01	0.01	0.01	0.01	0.01	0.01	0.01
Cr	0.01	0.01	0.01	0.00	0.00	0.00	0.00	0.00	0.00	0.00
Fe	0.46	0.44	0.46	0.49	0.46	0.49	0.50	0.46	0.51	0.48
Mn	0.01	0.01	0.01	0.01	0.01	0.01	0.01	0.01	0.01	0.01
Mg	1.48	1.50	1.51	1.48	1.50	1.47	1.47	1.51	1.45	1.49
Ca	0.05	0.04	0.03	0.03	0.03	0.03	0.04	0.03	0.04	0.03
Na	0.01	0.00	0.00	0.00	0.00	0.00	0.00	0.00	0.00	0.00
Total	4.01	4.01	4.01	4.01	4.01	4.01	4.02	4.01	4.02	4.01
Fe/Mn	33.5	33.1	33.9	35.7	33.7	35.7	38.5	33.3	35.7	35.3
Fe/Mg	0.31	0.29	0.31	0.33	0.31	0.34	0.34	0.31	0.34	0.32
Fs	23.6	22.6	23.6	24.9	23.7	25.3	25.3	23.7	26.1	24.5
Wo	2.3	1.9	1.6	1.5	1.7	1.5	2.0	1.7	2.1	1.7

Numbers in square brackets represent number of analyses averaged.
Numbers in parentheses represent 1σ precision of replicate analyses expressed as the least digit cited.

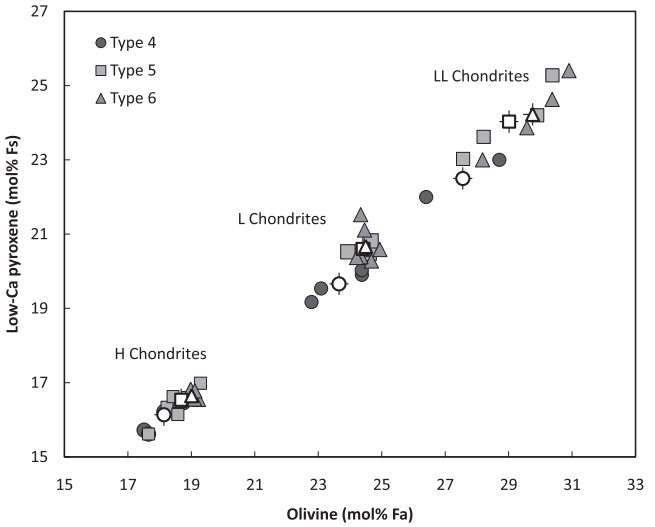

Fig. 3. Olivine (as mol% Fa) versus low-Ca pyroxene (as mol% Fs) in the H, L, and LL chondrites. Symbols are average analyses from each chondrite analyzed in this study; circles are type 4 chondrites, squares are type 5, and triangles are type 6. Overall averages of all samples at each petrologic type are shown as open symbols with crosshairs. 1σ standard deviations are smaller than the symbols.

pyroxene at each petrologic type are represented by open symbols. Although there is a small spread of Fa content among individual samples, mean Fa content in olivine and mean Fs content in low-Ca pyroxene increase with petrologic type in all three chondrite groups, which is in agreement with data from previous studies.

Redox state in the H, L, and LL chondrites can also be examined using molar Fe/Mn and molar Fe/Mg ratios in silicate minerals (Goodrich and Delany 2000). Fe addition (as a result of oxidation) is indicated by the presence of a linear trend, which passes through the origin (y-intercept = 0) and is defined by constant Mn/Mg ratios. Molar Fe/Mn ratios and molar Fe/Mg ratios in olivine and low-Ca pyroxene are listed in Tables 3–8. Figures 4a–c compare Fe/Mn ratios to molar Fe/Mg ratios in the H, L, and LL chondrites, respectively, to check for the presence of Fe addition trends. In the H and LL chondrites, linear regression analyses of data yield R^2 values ranging from 0.53 to 0.85. R^2 values and slopes do not change when the y-intercept is set at zero, indicating that data fall on lines that pass naturally through the origin (Figs. 4a and 4c). However, R^2 values are less than 0.90 in both groups, suggesting that there is a poor correlation between variables. In the L chondrites, R^2 values are 0.23 (in olivine) and 0.34 (in pyroxene) and R^2 values decrease significantly when the y-intercept is set at zero, indicating that the L chondrite data are best fit with a line that does not pass through the origin. In all three chondrite groups, there is considerable overlap between molar Fe/Mn and

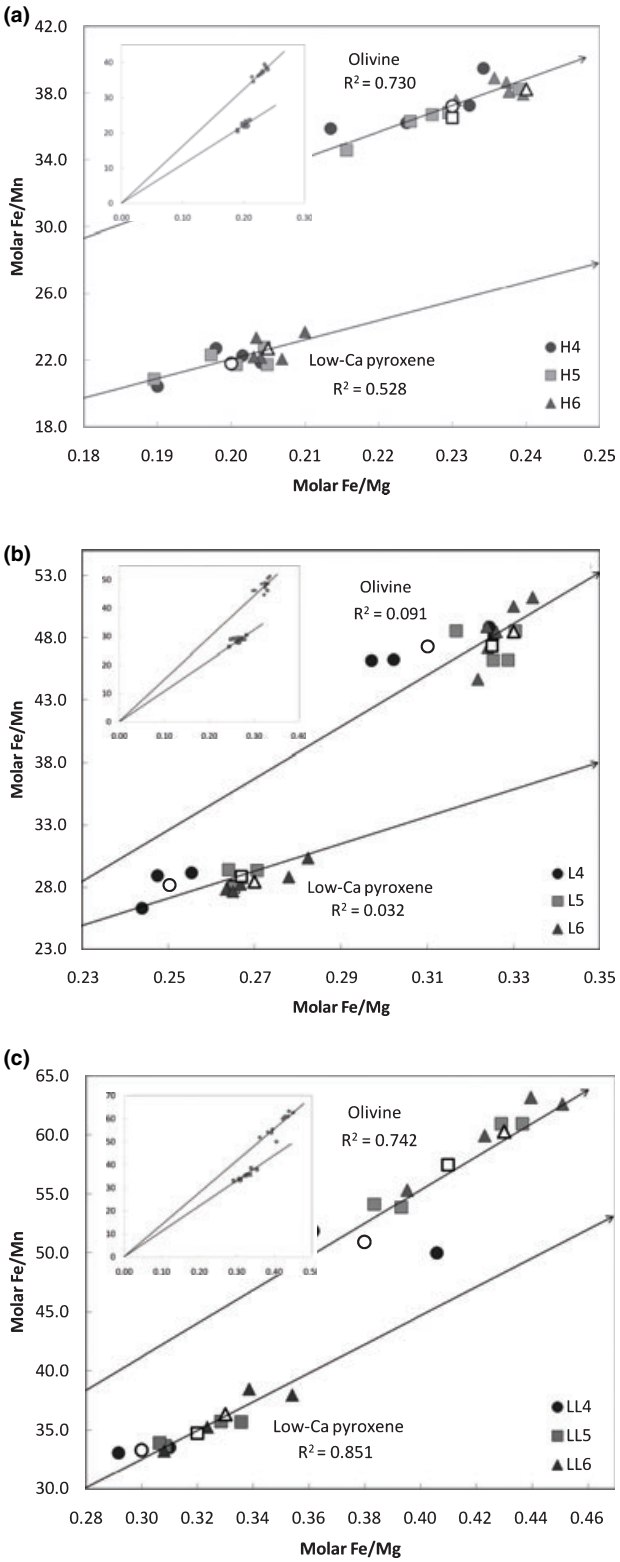

Fig. 4. Molar Fe/Mn versus Fe/Mg ratios for olivine and low-Ca pyroxene in (a) H, (b) L, and (c) LL chondrites. Solid symbols represent average analyses from each chondrite; Open symbols are averages for each petrologic type. Each inset shows a linear regression of data, where the y-intercept is zero.

Fe/Mg ratios at different petrologic types. However, averages of data at petrologic types 4, 5, and 6 generally plot in an Fe-enrichment sequence in all three chondrite groups.

Examination of mol% Fa, mol% Fs, and Mg/Fe versus Mn/Fe appears to suggest that the silicate minerals are being enriched in Fe during metamorphism in the H and LL chondrites. Data from the L chondrites, however, do not appear to support this assertion. Average mol% Fa versus mol% Fs values do not show an increase between petrologic type 5 and type 6, and Mg/Fe versus Mn/Fe data for the L chondrites do not fall on an Fe-enrichment trend. Oxidation trends in the L chondrites are expected, but have likely been erased by residual heating from an episode of extreme shock in the L chondrite parent body, which took place ~470 Ma (Anders 1964; Heymann 1967; Schmitz et al. 2003; Korochantseva et al. 2007). This shock event left many parts of the L chondrite parent body at high residual temperatures (up to 1500 °C) for weeks to months (Smith and Goldstein 1977). As a result, the expected metamorphic sequence (from type 4 to type 6) was interrupted and compositions of mineral phases were altered (i.e., Dodd and Jarosewich 1979; Huston and Lipschutz 1984), accounting for the lack of oxidation trends in the L chondrites.

Fe-Ni Metal Content and Oxygen Isotope Compositions

Additional mineralogical and chemical trends in metals have also been cited as evidence of progressive oxidation in the equilibrated ordinary chondrites. Rubin (1990) noted enrichment trends of Co and Ni in kamacite with increasing petrologic type, and McSween and Labotka (1993) observed an increase in mean ratios of Ni/Fe and Co/Fe in bulk metal. Although metals were not analyzed in this study, weight ratios of Ni/Fe and Co/Fe in 39 of our samples were determined from bulk chemical analyses collected by Jarosewich (1990). Mean ratios of Ni/Fe and Co/Fe are listed in Table 9 (along with standard deviations), and these data are presented graphically in Fig. 5. Although mean ratios of Ni/Fe and Co/Fe increase with petrologic type in the H chondrites, this is not the case in the L and LL chondrites. As suggested previously, the absence of a trend in the L chondrites is due to shock events in the parent body. In the LL chondrites, there is insufficient data to determine if Ni/Fe and Co/Fe increase with increasing metamorphic type, because only one LL4 and one LL5 sample were analyzed by Jarosewich (1990). Based on our data, it is unclear whether compositional ratios in metal support the oxidation hypothesis in all chondrite groups.

Oxygen isotopic compositions also change systematically with petrologic type, as mean $\delta^{18}O$ and $\delta^{17}O$ progressively decrease from type 4 to type 6 in all three chondrite groups (Clayton et al. 1991; Rubin 2005). This decrease in mean $\delta^{18}O$ and $\delta^{17}O$ correlates with increasing mol% Fa in olivine, suggesting that there is a correlation between oxygen isotope compositions and oxidation state (Rubin 2005). Rubin (2005) attributed the decreases in $\delta^{18}O$ and $\delta^{17}O$ with petrologic type to loss of chondritic water during thermal metamorphism. It has been suggested that chondritic water was enriched in heavy O isotopes (Choi et al. 1998). If this was the case, loss of water during progressive metamorphism would result in lower $\delta^{18}O$ and $\delta^{17}O$ values in chondrites of higher petrologic types (i.e., those that have lost more water through oxidation). Because oxygen isotope compositions have only been measured in seven of the chondrites analyzed in this study, we do not have sufficient data to address the relationship between oxygen isotopic compositions and oxidation. We believe,

Table 9. Mean weight ratios and standard deviations of bulk metal compositions from Jarosewich (1990).

Chondrite group	Ni/Fe	Standard deviation	Co/Fe	Standard deviation
H4	0.102	0.007	0.0043	0.0012
H5	0.108	0.011	0.0048	0.0012
H6	0.109	0.006	0.0054	0.0006
L4	0.177	0.021	0.0087	0.0013
L5	0.169	0.017	0.0086	0.0012
L6	0.189	0.030	0.0096	0.0012
LL4	0.346	ind.[a]	0.0160	ind.
LL5	0.883	ind.	0.0325	ind.
LL6	0.779	0.386	0.0354	0.0188

[a]Indeterminate, only one analysis available.

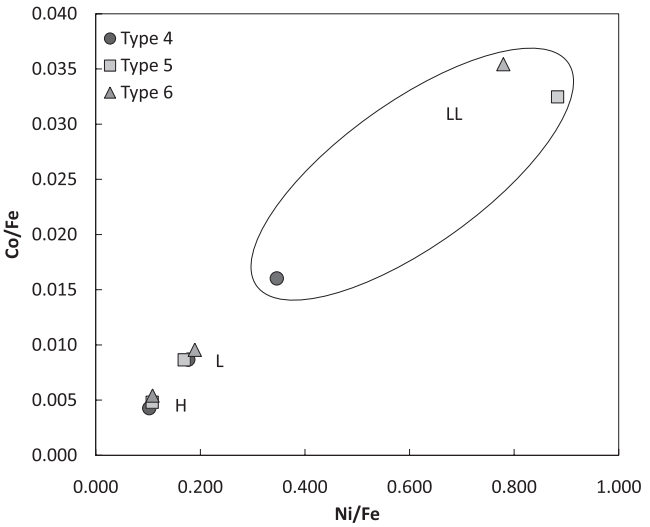

Fig. 5. Weight ratios of Ni/Fe and Co/Fe (from Jarosewich 1990) in 18 H, 15 L, and 6 LL chondrites analyzed in this study.

however, that data from Rubin (2005) strongly support the hypothesis that $\delta^{18}O$ and $\delta^{17}O$ decrease with increasing petrologic type as a result of progressive oxidation.

REDOX STATE IN ORDINARY CHONDRITE PARENT BODIES

Initial Reduction

Mineralogical and geochemical evidence seem to support the hypothesis that type 4–6 ordinary chondrites became progressively oxidized during metamorphism. The unequilibrated ordinary chondrites, however, appear to have experienced a very different redox history. Any model of redox state in the ordinary chondrite parent body would be incomplete without a discussion of redox state in the type 3 chondrites. The unequilibrated chondrites were not included as part of this study because the question of redox state in type 3.1–3.9 chondrites was addressed by Menzies et al. (2005). Using XRD and Mössbauer spectroscopy, Menzies et al. (2005) investigated the redox state in 21 unequilibrated ordinary chondrites and identified several mineralogical trends indicative of reduction. Based on their observations and on those of McSween and Labotka (1993), Menzies et al. (2005) suggested that unequilibrated chondrites experienced reduction until type 4 conditions were reached, at which time progressive oxidation began and continued until metamorphism ended (type 6). This model, however, does not apply to unequilibrated chondrites, such as Semarkona, which contain carbide-magnetite assemblages that form under oxidizing conditions (Krot et al. 1997). Although data suggest that reduction occurs in most type 3 chondrites, this is not the case in all unequilibrated chondrites.

The Menzies et al. (2005) model suggests that there must have been a sudden shift from a reducing to an oxidizing environment in the ordinary chondrite parent body. Though it may seem difficult to reconcile these contrasting environments, this shift may be a natural effect of known mineralogical changes that take place between unequilibrated and equilibrated chondrites, specifically the disappearance of carbon and phyllosilicates at type 4 conditions. Carbon, the most likely agent responsible for reduction (Brett and Sato 1984; Sears and Weeks 1986), decreases in abundance with progressive metamorphism in the unequilibrated chondrites (Grady et al. 1982) and disappears at temperatures equivalent to petrologic type 4 (Menzies et al. 2005). Brett and Sato (1984) also noted that carbon dissolves in Fe-Ni metal at high temperatures, so it is unlikely that carbon is a viable reducing agent past petrologic type 4. Phyllosilicates (hydrous phases common in unequilibrated chondrites) are also absent from equilibrated chondrites. In the unequilibrated chondrites, dehydration of hydrous phases converts Fe^{3+} in phyllosilicates to Fe^{2+} in olivine and pyroxene, which is then reduced to Fe^0 in metal (Menzies et al. 2005). When the hydrous phases disappear at type 4, the source of Fe^{3+} is removed from the system and reduction ceases. At petrologic type 4, there is no carbon available and all phyllosilicates have dehydrated, making Fe metal available for oxidation.

Origin of the Oxidizing Agent

While initial reduction appears to be driven by carbon, the most plausible agent responsible for oxidation in the ordinary chondrite parent bodies is an externally derived fluid, most likely in the vapor phase (McSween and Labotka 1993). Several lines of evidence indicate that aqueous fluid was present in unequilibrated ordinary chondrites, including the presence of minor alteration products, such as phyllosilicates and clay minerals (Hutchison et al. 1987; Alexander et al. 1989), and carbide-magnetite-sulfide veins cross-cutting fine-grained chondrule rims (Krot et al. 1997). Water-rich mesostases on the outer reaches of chondrule glass (Grossman and Brearley 2001) and magnetite grains showing large mass-dependent isotopic fractionation of oxygen ($\delta^{18}O \sim 13‰$) in type 3 chondrites (Choi et al. 1998) also indicate that water was present in ordinary chondrite parent bodies prior to metamorphism. Because fluid was presumably lost during metamorphism, evidence of water in type 4–6 ordinary chondrites is limited. However, the presence of bleached chondrules (products of low-temperature aqueous alteration) in type 4–6 chondrites (Grossman et al. 2000) indicates that fluid remained in the ordinary chondrite parent bodies throughout thermal metamorphism. Water has also been measured in recovered ordinary chondrites (Jarosewich 1990). However, it is unlikely that all of this water is indigenous, as some of it may have been absorbed from the terrestrial atmosphere.

Although there are several lines of evidence to suggest that aqueous fluid was present in the ordinary chondrite parent bodies, the origin of fluid in these bodies is unclear. McSween and Labotka (1993) suggested that the oxidizing fluid was produced by melting small amounts of ice, which accreted in different abundances on each of the three ordinary chondrite parent bodies. This model, however, does not account for the metal-silicate fractionation trend, which distinguishes the three ordinary chondrite groups, nor can it explain systematic changes in elemental composition (such as siderophile abundances and volatile/refractory ratios) that occur through the H–L–

LL sequence (Kallemeyn et al. 1989). The presence of ice on ordinary chondrite parent bodies is also problematic, as ordinary chondrite parent material is thought to have accreted inside the snow line at heliocentric distances where ice is not expected to form (Bell et al. 1989). However, it may have been possible to accrete ice on the ordinary chondrite parent bodies if the snow line was not static and migrated over time.

As an alternative hypothesis, Wasson (2000) suggested that water was incorporated as hydrous silicates. Phyllosilicates may have formed by direct condensation of a modified solar gas composition under optimal temperature conditions (Petaev and Wood 1998; Wasson and Trigo-Rodríguez 2004) or may have been produced in icy regions by shock waves (Ciesla et al. 2003) and been transported into inner regions by gas drag (Ciesla and Lauretta 2005). If phyllosilicates formed as the result of condensation followed by evaporation, the abundance of phyllosilicates among fine-grained nebular material may have increased over time (Wasson and Trigo-Rodríguez 2004). Rubin (2005) suggests that the H chondrites agglomerated first and incorporated the lowest abundances of hydrated silicates, while the LL chondrites, which agglomerated last, incorporated the highest abundance of phyllosilicates. As phyllosilicates agglomerated, $\Delta^{17}O$ became progressively heavier, accounting for the increase in oxidation states from the Hs to the LLs (Rubin 2005).

Neither of these hypotheses can account for our observation that the type 6 chondrites experienced a higher degree of oxidation than the type 4 chondrites and apparently required a larger amount of the oxidizing agent. In the onion-shell model of the ordinary chondrite parent bodies, the inner-most region corresponds to the highest temperatures (petrologic type 6) and the outer region to the lowest temperatures (petrologic type 3). Melting accreted ice could have served as a source of water for type 3 (and possibly type 4) material, but it is unlikely that melted ice would have provided a substantial amount of water to type 5 and 6 material deeper in the parent body. Even if water percolated through the parent body by some mechanism, possibly along a system fractures, it is unlikely that more water would have reached the interior of the body than the surface.

The phyllosilicate hypothesis also fails to account for the increase in oxidation from type 4 to type 6. If the abundance of phyllosilicates in nebular material increased over time, as suggested by Wasson and Trigo-Rodríguez (2004), material that accreted first (type 6) would contain less phyllosilicates (and less water) than material that accreted later (type 3). However, if we eliminate the suggestion that phyllosilicate abundances in nebular material increased over time, we can assume that the parent body accreted from homogeneous material. If this was the case, phyllosilicates would have been equally distributed throughout the parent body prior to metamorphism. If all water was released by progressive dehydration of hydrous silicate minerals prior to type 4 conditions, water would have been evenly distributed as well, and the amount of oxidizing agent available for oxidation would not vary.

If water was distributed homogeneously throughout the parent body, then the abundance of water may not be the only factor driving the oxidation reaction in the parent body. Temperature also plays a significant role in oxidation, as higher temperatures favor a more rapid and extensive reaction. As oxidation occurs during progressive metamorphism (i.e., as heating progresses), it is very likely that oxidation is driven by increasing temperature. Therefore, it is possible that the increase in oxidation from type 4 to type 6 may not require a larger amount of oxidizing agent, but may instead reflect more advanced oxidation at higher temperatures. The kinetics of the reaction may also be a factor in the degree of oxidation. It is possible that the activation energy required to initiate the oxidation reaction is barely attained in type 4, resulting in only a small amount of oxidation. Once the activation energy has been reached, the reaction may progress to completion, depending on the rate of the reaction.

Abundance of Fluid Required for Oxidation

As a result of the continuous reaction enstatite + Fe + O_2 = olivine, there are measurable changes in silicate abundances of the equilibrated chondrites during progressive metamorphism. If we assume the observed changes in mineral abundances are caused by interactions between the fluid and the meteorite, we can estimate the minimum amount of fluid necessary to oxidize Fe in chondrites using a mass balance of the oxidation equation. The change in the amount of O (expressed here as H_2O) is the amount necessary to convert mean mineral abundances of olivine and pyroxene in type 4 to those in type 6. As a precondition for mass balance of the oxidation equation, we assume that the bulk composition remains constant and the weights of Si, Fe, Mg, and Ni + Co are conserved. Changes in abundances determined using mass balance are presented in Table 10, along with actual measured abundances low-Ca pyroxene, olivine, and metallic Fe.

Using the difference between mean low-Ca pyroxene in type 4 and mean low-Ca pyroxene in type 6, we can determine the decrease in metallic Fe, increase in olivine, and amount of H_2O required to balance the oxidation equation. In the H chondrites, the measured decrease in low-Ca pyroxene (2.1 wt%) is balanced by a 3.6 wt%

Table 10. Measured and mass balanced changes in abundances from petrologic type 4–6.

	Measured decrease in low-Ca pyroxene	Decrease in metallic Fe		Increase in olivine		
		Balanced	Measured	Balanced	Measured	H_2O required
H4–H6	2.1	1.2	1.6	3.6	5.9	0.4
L4–L6	1.9	1.1	0.4	3.3	2.3	0.3
LL4–LL6	3.7	2.1	1.2	6.4	2.8	0.7

Values are in wt%.

increase in olivine, a 1.2 wt% decrease in metallic Fe, and requires 0.4 wt% H_2O. In L chondrites, a 1.9 wt% difference between low-Ca pyroxene in type 4 and type 6 is balanced by a 3.3 wt% increase in olivine, a 1.1 wt% decrease in metallic Fe, and consumes 0.3 wt% water. Mass balance of type 4 abundances in the LL chondrites produces 6.4 wt% olivine, consumes 2.1 wt% metallic Fe, and requires 0.7 wt% water.

Phase abundances determined using mass balance of the oxidation equation do not always correlate with measured phase changes. In the H chondrites, measured changes in olivine and Fe metal are slightly higher than mass balance values (by 0.4 wt% in metal and 2.3 wt% in olivine). The converse is true in the L and LL chondrites, as measured abundance changes are lower than those calculated using mass balance. In the L chondrites, measured changes in abundances are 0.7 wt% lower in metal and 1.0 wt% lower in olivine. In the LL chondrites, the difference between measured and mass balance-derived abundances is 0.9 wt% in metal and 3.6 wt% in olivine. Mass balance calculations should accurately model expected phase changes, and the inconsistency between XRD-measured abundance changes and those calculated using mass balance may be a consequence of the error associated with the XRD technique. Despite this error, it is clear that the amount of water required is minimal.

Based on mass balance in the H and L chondrites, the amount of water required to convert low-Ca pyroxene to olivine is between 0.3 and 0.4 wt%. In the LL chondrites, this abundance is 0.7 wt%. However, we believe that the measured decrease in low-Ca-pyroxene in the LL chondrites is too large, resulting in more water than expected being consumed during mass balance. It is more likely the abundance of water required for oxidation in the LL chondrites is also in the range of 0.3–0.4 wt%. These abundances are slightly higher than those suggested by McSween and Labotka (1993) (0.1 wt% in the H chondrites and 0.2 wt% in the L chondrites). It is important to note we have assumed all O is present as H_2O, although the fluid likely contained other oxygenated (CO and CO_2) and non-oxygenated species (CH_4 or H_2) (McSween and Labotka 1993). As a result, these calculated abundances are minimum values.

EVALUATION OF PYROXENE AND PLAGIOCLASE GEOTHERMOMETRY

Plagioclase Modal Abundances

Unlike olivine and low-Ca pyroxene abundances, plagioclase abundances do not show any systematic changes with increasing petrologic type. However, as in the case of olivine and low-Ca pyroxene, the presence or absence of trends may be obscured by the error of the XRD-technique. Average plagioclase abundances vary slightly from the H to LL chondrites (from 9.0 ± 0.5 wt% in the Hs, to 9.4 ± 0.8 wt% in the Ls, to 9.7 ± 0.8 wt% in the LLs). Table 2 lists average plagioclase abundances and standard deviations, while Fig. 6 illustrates plagioclase abundances as a function of petrologic type. Although normative plagioclase abundances increase from petrologic type 4 to type 6, the absence of an equivalent trend in modal abundances indicates that plagioclase abundances do not change with increasing petrologic type. This is contrary to petrologic observations from previous studies (Van Schmus and Wood 1967; Sears et al. 1980), which suggest that plagioclase continues to crystallize through type 5 conditions. These new data may instead indicate

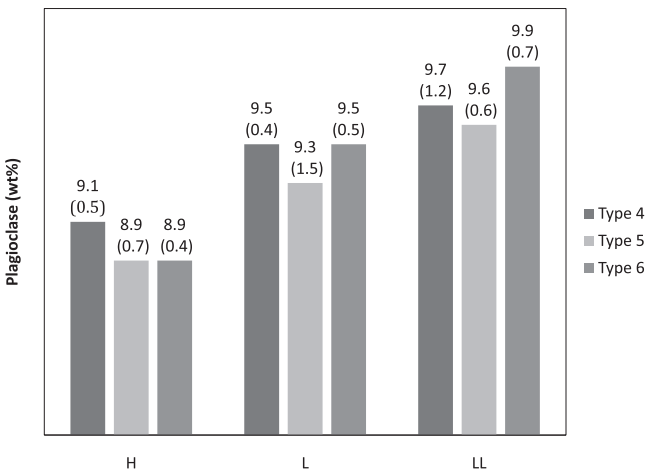

Fig. 6. XRD-measured modal abundances (wt%) of plagioclase in the H, L, and LL chondrites at petrologic types 4, 5, and 6. 1σ standard deviations are in parentheses.

that plagioclase undergoes grain growth, rather than crystallization, with increasing metamorphic grade.

Gastineau-Lyons et al. (2002) suggested that the timing of plagioclase crystallization could be constrained by comparing normative and modal plagioclase abundances, which should converge when all available chondrule glass has recrystallized. A comparison of normative plagioclase abundances (McSween et al. 1991) with modal abundances of type 3 chondrites (Menzies et al. 2005) and type 4–6 chondrites (Dunn et al. 2009) is shown in Fig. 7. Although modal and normative values do not converge absolutely, values converge at type 4 in the H and L chondrites and at type 5 in the LL chondrites when 1σ standard deviations are considered (Fig. 7). Our assessment of modal and normative plagioclase abundances yields a slightly different conclusion from that of Gastineau-Lyons et al. (2002), who examined plagioclase abundances in equilibrated L and LL chondrites. In Gastineau-Lyons et al. (2002), normative and modal plagioclase abundances did not converge until petrologic type 6 in the L chondrites and type 5 in the LLs. However, observations in the Gastineau-Lyons et al. (2002) study were based on a single chondrite of each petrologic type and do not represent a statistically significant sampling of the L and LL chondrite groups. Based on the observations from this study, we suggest that chondrule glass crystallized to form plagioclase by type 4 temperature conditions in the H and L chondrites. In the LL chondrites, plagioclase appears to have crystallized from chondrule glass by type 5 conditions. Additional normative abundances of the LL4 and LL5 chondrites may indicate that chondrule glass crystallized into plagioclase by type 4 in the LL chondrites.

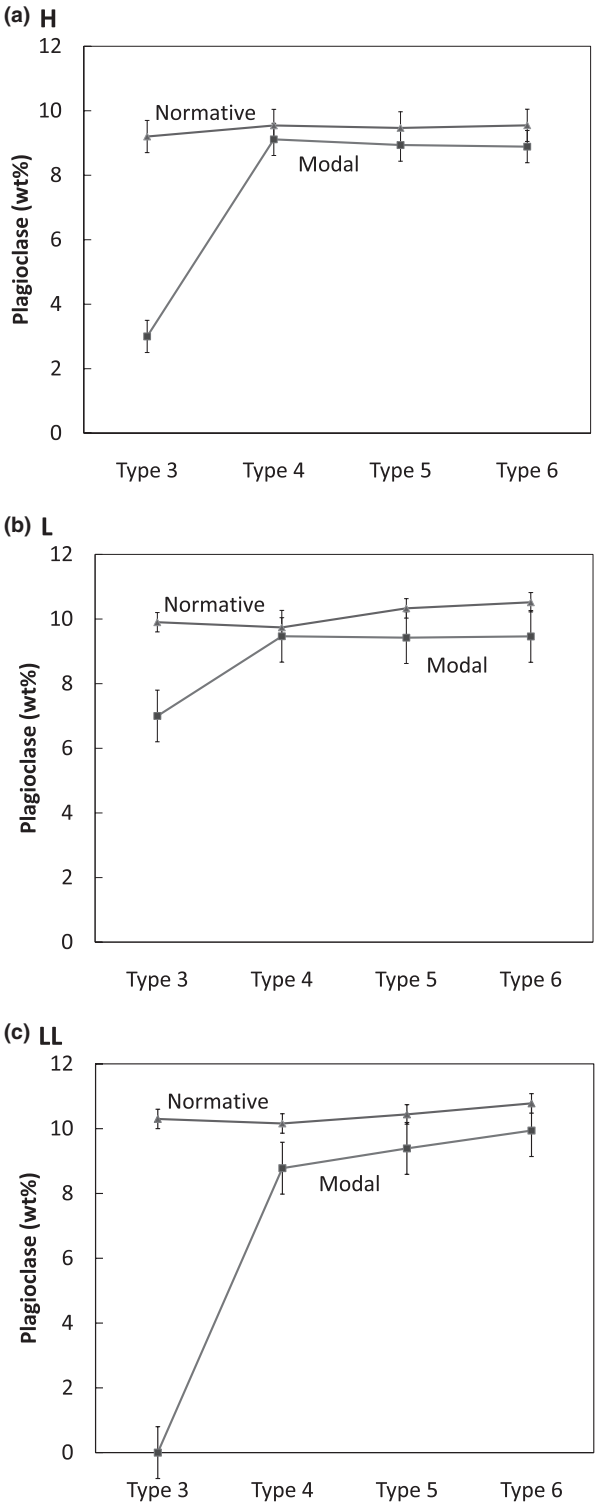

Fig. 7. XRD-measured modal plagioclase abundances for the (a) H, (b) L, and (c) LL chondrites plotted against normative plagioclase abundances from McSween et al. (1991). Type 3 modal abundances are from Menzies et al. (2005). Standard deviations of modal plagioclase abundances are listed in Table 2. 1σ standard deviations for type 3 chondrites are 0.5 wt% for the Hs and 0.3 wt% for the Ls and LL.

Peak Temperature Estimates

While most traditional thermometers are based on cation exchange, the plagioclase thermometer (Nakamuta and Motomura 1999) is based on the distribution of Si and Al in the unit cell of plagioclase, which is directly linked to temperature. In plagioclase that crystallizes at lower temperatures, Al is concentrated in a single tetrahedral site (ordered); at higher temperatures, Al is distributed among all four sites (disordered). Nakamuta and Motomura (1999) suggest that the transition from ordered to disordered occurs at temperatures >850 °C. However, measured thermoluminescence sensitivity of feldspars indicates that this transition occurs at lower temperatures, by petrologic type 3.5 (Sears et al. 1982; Benoit et al. 2001, 2002). The validity of using the plagioclase thermometer to determine peak temperatures rests on the assumption that plagioclase continued to crystallize through type 6 conditions (Nakamuta and

Motomura 1999). Our data indicate that crystallization was complete much earlier in the metamorphic sequence, and we suggest that the plagioclase thermometer should not be used to determine peak metamorphic temperatures in ordinary chondrites. Pyroxene thermometry provides more accurate estimates of the peak temperatures reached in ordinary chondrite parent bodies.

To assess peak metamorphic temperatures in ordinary chondrite parent bodies, we performed pyroxene thermometry on nine type 6 ordinary chondrites using QUILF95 (Anderson et al. 1993; modified for Windows 95), a computer model based on the graphical approach of Lindsley (1983). Type 4 and 5 chondrites were not examined because type 6 chondrites represent the highest degree of metamorphism and therefore record the highest temperatures reached in the parent body. QUILF95 incorporates improved experimental data for pyroxene equilibrium, eliminates errors associated with converting and plotting chemical analyses on the pyroxene quadrilateral, and eliminates difficulties associated with discerning temperature differences. Temperatures were calculated at a pressure of 1 bar. Average high-Ca pyroxene analyses used to calculate peak temperatures are listed in Table 11.

Peak temperature estimates for low-Ca pyroxene and high-Ca pyroxene pairs are presented in Table 12. Peak temperatures range from 866 ± 63 °C to 967 ± 25 °C, with all but two temperatures below the Fe-Ni metal-FeS eutectic (950 °C). (Because chondrites did not experience melting or differentiation, peak temperatures should be below this eutectic.) Temperatures above 950 °C may be higher than expected due to inadequate high-Ca pyroxene analyses. There is no appreciable difference in temperature estimates from each chondrite group, and peak temperatures overlap between groups, suggesting that observations of lower temperatures in the H chondrites (Olsen and Bunch 1984; Nakamuta and Motomura 1999) are inaccurate. The QUILF95 program yields an uncertainty of ±50 °C for temperatures calculated from low-Ca pyroxene and high-Ca pyroxene pairs. The actual error can be larger if equilibrium has not been reached between the two pyroxene compositions. Because the calculated error in the model does not account for analytical error, we also determined the maximum temperature range due to analytical uncertainty. Minimum and maximum temperatures were calculated by increasing or decreasing the amount of CaO (the most sensitive component in the temperature determinations) by an amount equal to the 1σ standard deviation of low-Ca pyroxene and high-Ca pyroxene. All temperatures calculated from pyroxene pairs fall within the temperature range due to expected analytical error.

Table 11. Average electron microprobe analyses for high-Ca pyroxene in type 6 chondrites.

	Butsura H6 [3]	Ipiranga H6 [1]	Karkh L6 [13]	Kunashak L6 [1]	Kyushu L6 [1]	Bandong LL6 [3]	Cherokee Springs LL6 [4]	Karatu LL6 [8]	St. Severin LL6 [3]
SiO_2	54.6 (13)	54.8	53.4 (2)	54.0	53.4	53.1 (8)	53.7 (3)	53.5 (3)	53.4 (3)
TiO_2	0.44 (3)	0.51	0.49 (2)	0.47	0.51	0.49 (3)	0.44 (3)	0.46 (3)	0.43 (5)
Al_2O_3	1.32 (77)	0.50	0.51 (2)	0.50	0.52	0.90 (39)	0.53 (9)	0.56 (10)	0.50 (3)
Cr_2O_3	0.75 (3)	0.80	0.88 (46)	0.91	0.98	0.91 (2)	0.66 (8)	0.82 (6)	0.79 (11)
FeO	4.44 (12)	3.42	5.05 (18)	5.14	4.97	6.51 (59)	4.96 (16)	6.76 (28)	6.47 (36)
MnO	0.24 (1)	0.18	0.24 (2)	0.24	0.23	0.29 (4)	0.21 (6)	0.24 (3)	0.22 (4)
MgO	16.5 (4)	17.2	16.7 (1)	16.9	16.7	16.3 (2)	16.6 (1)	16.3 (2)	16.4 (1)
CaO	21.6 (5)	23.0	21.9 (1)	21.1	21.7	20.7 (6)	22.1 (3)	21.0 (3)	21.3 (5)
Na_2O	0.64 (2)	0.54	0.59 (1)	0.60	0.57	0.61 (3)	0.53 (7)	0.55 (3)	0.50 (6)
Total	100.5	101.1	99.7	99.9	99.6	99.9	99.7	100.1	100.1
Cations based on 6 oxygens									
Si	1.98	1.98	1.97	1.98	1.97	1.96	1.98	1.97	1.97
Ti	0.01	0.01	0.01	0.01	0.01	0.01	0.01	0.01	0.01
Al	0.06	0.02	0.02	0.02	0.02	0.04	0.02	0.02	0.02
Cr	0.02	0.02	0.03	0.03	0.03	0.03	0.02	0.02	0.02
Fe	0.14	0.10	0.16	0.16	0.15	0.20	0.15	0.21	0.20
Mn	0.01	0.01	0.01	0.01	0.01	0.01	0.01	0.01	0.01
Mg	0.89	0.93	0.92	0.93	0.92	0.90	0.91	0.89	0.90
Ca	0.84	0.89	0.86	0.83	0.86	0.82	0.87	0.83	0.84
Na	0.05	0.04	0.04	0.04	0.04	0.04	0.04	0.04	0.04
Total	3.99	4.00	4.01	4.00	4.01	4.01	4.01	4.01	4.01
Fs	7.6	5.7	8.4	8.6	8.3	10.9	8.2	11.1	10.6
Wo	44.8	46.2	44.5	43.2	44.3	42.5	44.9	42.7	43.2

Numbers in square brackets represent number of analyses averaged.
Numbers in parentheses represent 1σ precision expressed as the least digit cited.

Table 12. Peak metamorphic temperatures (°C) calculated from average low- and high-Ca pyroxene compositions.

		Pyroxene pairs	Maximum T Cpx − 1σ CaO Opx + 1σ CaO		Minimum T Cpx + 1σ CaO Opx − 1σ CaO
Butsura	H6	929 ± 20	950 ± 15		894 ± 20
Ipiranga	H6	866 ± 63		Indeterminate[a]	
Karkh	L6	967 ± 25	1022 ± 38		896 ± 15
Kunashak	L6	964 ± 39		Indeterminate	
Kyushu	L6	894 ± 64		Indeterminate	
Bandong	LL6	933 ± 50	984 ± 41		888 ± 70
Cherokee Springs	LL6	876 ± 66	910 ± 64		837 ± 66
Karatu	LL6	945 ± 44	974 ± 39		916 ± 49
St. Severin	LL6	904 ± 35	934 ± 24		884 ± 49

[a]Only one cpx analysis available.

Slater-Reynolds and McSween (2005) used QUILF95 to calculate peak temperatures of 41 type 6 ordinary chondrites. Of the nine chondrites analyzed in this study, two (Kyushu and Saint Séverin) were also analyzed by Slater-Reynolds and McSween (2005). The remaining seven chondrites add to the database of peak temperatures estimated from pyroxene thermometry. Temperatures calculated in this study for Kyushu and Saint Séverin are higher than those determined by Slater-Reynolds and McSween (2005). However, most of our estimated temperatures fall within the temperature range (812–945 °C) established by Slater-Reynolds and McSween (2005). Peak temperatures calculated in this study also agree with those determined using oxygen isotopes, which average 900 ± 50 °C (Clayton 1993). Our calculated peak temperatures are consistently higher than those determined using olivine-spinel thermometry (Kessel et al. 2007). However, olivine-spinel thermometry yields temperatures that are lower than expected due to continued Fe-Mg exchange between olivine and spinel during cooling. Like Slater-Reynolds and McSween (2005), our peak temperatures are also higher than those determined using plagioclase thermometry (Nakamuta and Motomura 1999). We suggest that the plagioclase-derived temperatures are not representative of peak conditions because plagioclase does not continue to crystallize through type 6 conditions.

CONCLUSIONS

In this study we evaluated oxidation state and peak temperatures in equilibrated ordinary chondrites using mineral abundances determined using powder XRD and supplemental chemical analyses. Based on our results, we suggest that oxidation occurred during progressive metamorphism of the equilibrated chondrites, and we cite the following observations as evidence:

1. Modal abundances of olivine and low-Ca pyroxene exhibit subtle but systematic changes between petrologic type 4 and type 6, and Ol/Opx ratios increase from type 4 to type 6 in both normative and modal data. Both trends suggest that olivine was produced at the expense of pyroxene during progressive metamorphism.
2. In all three chondrite groups, mean Fa in olivine and mean Fs in low-Ca pyroxene increase with increasing petrologic type, indicating that silicate phases became progressively enriched in Fe as a result of oxidation.
3. Linear trends indicative of Fe addition in silicate minerals appear to be present in the H and LL chondrites, though not in the L chondrites. Although there is considerable overlap between data at different petrologic types, values generally plot in an Fe-enrichment sequence. Individual data are too variable to constitute convincing evidence for or against oxidation in the L chondrites.
4. Mean ratios of Ni/Fe and Co/Fe in bulk metal increase with petrologic type in the H chondrites. An increasing trend is also discernable in the L chondrites when standard deviations are considered; however, a trend cannot be distinguished in the LL chondrites due to limited sampling in the LL4s and LL5s.

Prior to oxidation, which began at petrologic type 4 conditions, the ordinary chondrite parent bodies experienced a period of reduction (McSween and Labotka 1993; Menzies et al. 2005) that was driven by carbon, either as graphite or CO gas (Brett and Sato 1984; Sears and Weeks 1986). The most plausible agent responsible for oxidation in the ordinary chondrite parent bodies is an aqueous fluid, which was incorporated as hydrous silicates (Wasson 2000) and distributed homogeneously throughout the parent body. During oxidation, low-Ca pyroxene reacted with Fe^{2+}, released

by oxidation of Fe-Ni metal, to produce olivine as the oxidizing fluid is consumed. Based on mass balance of the oxidation equation, a minimum of 0.3–0.4 wt% H_2O was necessary to convert measured mineral abundances in type 4 chondrites to those in type 6.

Average plagioclase abundances increase slightly from the H to LL chondrites, but do not show any recognizable trends with petrologic type. Based on this observation and on a comparison of modal and normative plagioclase abundances, we suggest that plagioclase completely crystallized from glass by type 4 temperature conditions in the H and L chondrites and by type 5 in the LL chondrites. It is possible that plagioclase crystallization was complete at a lower petrologic grade in the LLs, but this cannot be determined based on available data. Because the validity of using the plagioclase thermometer to determine peak temperatures rests on the assumption that plagioclase continued to crystallize through type 6 conditions, we suggest that temperatures calculated using pyroxene goethermometry provide more accurate estimates of the peak temperatures reached in ordinary chondrite parent bodies. Peak temperatures calculated using QUILF95 range from 866 ± 63 ° to 967 ± 25 °C, and there is no appreciable difference in temperature estimates from each chondrite group.

Acknowledgments—We thank the Mineralogy Department at the Natural History Museum in London for the use of their facilities and for providing samples. Thanks to the Smithsonian Institution for providing thin sections and powders of the majority of samples examined in this study and to Allan Patchen at the University of Tennessee for his guidance using the electron microprobe. The authors also greatly appreciate the thoughtful comments of reviewers Derek Sears, Alan Rubin, and Adrian Brearley. This work was supported by NASA through Cosmochemistry grant NNG06GG36G to H. Y. M.

Editorial Handling—Dr. Adrian Brearley

REFERENCES

Afiattalab F. and Wasson J. T. 1980. Composition of the metal phases in ordinary chondrites: Implications regarding classification and metamorphism. *Geochimica et Cosmochimica Acta* 44:431–446.

Alexander C. M., Barber D. J., and Hutchison R. 1989. The microstructure of Semarkona and Bishunpur. *Geochimica et Cosmochimica Acta* 53:3045–3057.

Anders E. 1964. Origin, age, and composition of meteorites. *Space Science Reviews* 3:583–714.

Anderson D. J., Lindsley D. H., and Davidson P. M. 1993. QUILF: A Pascal program to assess equilibria among Fe-Mg-Mn-Ti oxides, pyroxenes, olivine, and quartz. *Computers and Geosciences* 19:1333–1350.

Batchelder M. and Cressey G. 1998. Rapid, accurate phase quantification of clay-bearing samples using a position sensitive X-ray detector. *Clays and Clay Minerals* 46:183–194.

Bell J. F., Davis D. R., Hartmann W. K., and Gaffey M. J. 1989. Asteroids: The big picture. In *Asteroids II*, edited by Binzel R. P., Gehrels T., and Matthews M. Tucson, AZ: The University of Arizona Press. pp. 921–945.

Benoit P. H., Hartmetz C. P., Batchelor J. D., Symes S. J. K., and Sears D. W. G. 2001. The induced thermoluminescence and thermal history and plagioclase feldspars. *American Mineralogist* 86:780–789.

Benoit P. H., Akridge G. A., Ninagawa K., and Sears D. W. G. 2002. Thermoluminescence sensitivity and thermal history of type 3 ordinary chondrites: Eleven new type 3.0–3.1 chondrites and possible explanation for differences among H, L, and LL chondrites. *Meteoritics & Planetary Science* 37:793–805.

Bland P. A., Cressey G., and Menzies O. N. 2004. Modal mineralogies of carbonaceous chondrites by X-ray diffraction and Mössbauer spectroscopy. *Meteoritics & Planetary Science* 39:3–16.

Brett R. and Sato M. 1984. Intrinsic oxygen fugacity measurements on seven chondrites, a pallasite, and tektite and the redox state of meteorite parent bodies. *Geochimica et Cosmochimica Acta* 48:111–120.

Burbine T. H., McCoy T. J., Jarosewich E., and Sunshine J. M. 2003. Deriving asteroid mineralogies from reflectance spectra: Implications for the MUSES-C target asteroid. *Antarctic Meteorite Research* 16:185–195.

Choi B. G., McKeegan K. D., Krot A. N., and Wasson J. T. 1998. Extreme oxygen isotope compositions in magnetite from unequilibrated ordinary chondrites. *Nature* 392:577–579.

Ciesla F. and Lauretta D. 2005. Radial migration and dehydration of phyllosilicates in the solar nebula. *Earth and Planetary Science Letters* 231:1–8.

Ciesla F., Lauretta D. S., Cohen B. A., and Hood L. L. 2003. A nebular origin for chondritic fine-grained phyllosilicates. *Science* 299:549–552.

Clayton R. N. 1993. Oxygen isotopes in meteorites. *Annual Review of Earth and Planetary Sciences* 21:115–149.

Clayton R. N., Mayeda T. K., Goswami J. N., and Olsen E. J. 1991. Oxygen isotope studies of ordinary chondrites. *Geochimica et Cosmochimica Acta* 55:2317–2337.

Cressey G. and Schofield P. F. 1996. Rapid whole-pattern profile stripping methods for the quantification of multiphase samples. *Powder Diffraction* 11:35–39.

Dodd R. T. Jr. and Jarosewich E. 1979. Incipient melting in and shock classification of L-group chondrites. *Earth and Planetary Science Letters* 44:335–340.

Dodd R. T. Jr., Van Schmus W. R., and Koffman D. M. 1967. A survey of unequilibrated ordinary chondrites. *Geochimica et Cosmochimica Acta* 31:921–934.

Dunn T. L., Cressey G., McSween H. Y. Jr., and McCoy T. J. 2010. Analysis of ordinary chondrites using powder X-ray diffraction: 1. Modal mineral abundances. *Meteoritics & Planetary Science* 45:

Gastineau-Lyons H. K., McSween H. Y. Jr., and Gaffey M. J. 2002. A critical evaluation of oxidation versus reduction during metamorphism of L and LL group chondrites, and implications for asteroid spectroscopy. *Meteoritics & Planetary Science* 37:75–89.

Goodrich C. A. and Delany J. S. 2000. Fe/Mg-Fe/Mn relations in meteorites and primary heterogeneity in primitive achondrite parent bodies. *Geochimica et Cosmochimica Acta* 64:149–160.

Grady M. M., Swart P. K., and Pillinger C. T. 1982. Carbon isotopic composition of some type 3 ordinary chondrites (abstract). 13th Lunar and Planetary Science Conference. pp. 277–278.

Grossman J. N. and Brearley A. J. 2001. Chondrules with inhomogeneous mesostasis in highly unequilibrated ordinary chondrites: Further evidence for secondary processing of chondrules (abstract #1171). 32nd Lunar and Planetary Science Conference. CD-ROM.

Grossman J. N., Alexander C. M., Wang J., and Brearley A. J. 2000. Bleached chondrules: Evidence for widespread aqueous processes on the parent bodies or ordinary chondrites. *Meteoritics & Planetary Science* 35:467–486.

Heymann D. 1967. On the origin of hypersthene chondrites: Ages and shock effects of black chondrites. *Icarus* 6:189–221.

Huston T. J. and Lipschutz M. E. 1984. Chemical studies of L chondrites. III—Mobile trace elements and Ar-40/Ar-39 ages. *Geochimica et Cosmochimica Acta* 48:1319–1329.

Hutchison R., Alexander C. M., and Barber D. J. 1987. The Semarkona meteorite: First occurrence of smectite in ordinary chondrites and its implications. *Geochimica et Cosmochimica Acta* 51:1875–1882.

Jarosewich E. 1990. Chemical analyses of meteorites: A compilation of stony and iron meteorite analyses. *Meteoritics* 25:323–337.

Jones R. H. 1997. Equilibration of pyroxenes in type 4–6 LL chondrites (abstract). 28th Lunar and Planetary Science Conference. pp. 681–682.

Kallemeyn G. W., Rubin A. E., Wand D., and Wasson J. T. 1989. Ordinary chondrites: Bulk compositions, classification, lithophile-element fractionations and composition-petrographic type relationships. *Geochimica et Cosmochimica Acta* 53:2747–2767.

Keil K. and Fredriksson K. 1964. The iron, magnesium, and calcium distribution in coexisting olivines and rhombic pyroxenes of chondrites. *Journal of Geophysical Research* 69:3487–3515.

Kessel R., Beckett J. R., and Stolper E. M. 2007. The thermal history of equilibrated ordinary chondrites and the relationship between textural maturity and temperature. *Geochimica et Cosmochimica Acta* 71:1855–1881.

Korochantseva E. V., Trieloff M., Lorenz C. A., Buykin A. I., Ivanova M. A., Schwarz W. H., Hopp J., and Jessberger E. K. 2007. L-chondrite asteroid breakup tried to Ordovician meteorite shower by multiple isochron ^{40}Ar-^{39}Ar dating. *Meteoritics & Planetary Science* 42:113–130.

Kretz R. 1982. Transfer and exchange equilibria in a portion of the pyroxene quadrilateral as deduced from natural and experimental data. *Geochimica Cosmochimica Acta* 46:411–422.

Krot A. N., Zolensky M. E., Wasson J. T., Scott E. R. D., Keil K., and Ohsumi K. 1997. Carbide- magnetite assemblages in type 3 ordinary chondrites. *Geochimica et Cosmochimica Acta* 61:219–237.

Lindsley D. H. 1983. Pyroxene thermometry. *American Mineralogist* 68:477–493.

Mason B. 1963. Olivine compositions in ordinary chondrites. *Geochimica et Cosmochimica Acta* 27:1011–1024.

McSween H. Y. Jr. and Labotka T. C. 1993. Oxidation during metamorphism of the ordinary chondrites. *Geochimica et Cosmochimica Acta* 57:1105–1114.

McSween H. Y. Jr. and Patchen A. D. 1989. Pyroxene thermobarometry in LL-group chondrites and implications for parent body metamorphism. *Meteoritics* 24:219–226.

McSween H. Y. Jr., Sears D. W. G., and Dodd R. T. 1988. Thermal metamorphism. In *Meteorites and the early solar system*, edited by Kerridge J. F. and Matthews M. S. Tucson, AZ: The University of Arizona Press. pp. 102–113.

McSween H. Y. Jr., Bennett M. E., and Jarosewich E. 1991. The mineralogy of ordinary chondrites and implications for asteroid spectrophotometry. *Icarus* 90:107–116.

McSween H. Y. Jr., Ghosh A., Grimm R. E., Wilson L., and Young E. D. 2002. Thermal evolution of asteroids. In *Asteroids III*, edited by Bottke W. F. Jr., Cellino A., Paolicchi P., and Binzel R. P. Tucson, AZ: The University of Arizona Press. pp. 559–570.

Menzies O. N., Bland P. A., Berry F. J., and Cressey G. A. 2005. Mössbauer spectroscopy and X-ray diffraction study of ordinary chondrites: Quantification of modal mineralogy and implications for redox conditions during metamorphism. *Meteoritics & Planetary Science* 40:1023–1042.

Nakamuta Y. and Motomura Y. 1999. Sodic plagioclase of type 6 ordinary chondrites: Implications for the thermal histories of parent bodies. *Meteoritics & Planetary Science* 34:763–772.

Olsen E. J. and Bunch T. E. 1984. Equilibrium temperatures of the ordinary chondrites: A new evaluation. *Geochimica Cosmochimica Acta* 48:1363–1365.

Petaev M. I. and Wood J. A. 1998. The condensation with partial isolation model of condensation in the solar nebula. *Meteoritics & Planetary Science* 33:1123–1137.

Rubin A. E. 1990. Kamacite and olivine in ordinary chondrites: Intergroup and intragroup variations. *Geochimica et Cosmochimica Acta* 54:1217–1232.

Rubin A. E. 2005. Relationships among intrinsic properties of ordinary chondrites: Oxidation state, bulk chemistry, oxygen-isotopic composition, petrologic type, and chondrule size. *Geochimica et Cosmochimica Acta* 69: 4907–4918.

Schmitz B., Häggström T., and Tassinari M. 2003. Sediment-dispersed extraterrestrial chromite traces a major asteroid disruption event. *Science* 300:961–964.

Scott E. R. D., Taylor G. J., and Keil K. 1986. Accretion, metamorphism and brecciation of ordinary chondrites: Evidence from petrologic studies of meteorites from Roosevelt County, New Mexico. *Journal of Geophysical Research* 91:E115–E123.

Sears D. W. G. and Weeks K. S. 1986. Chemical and physical studies of type 3 chondrites: VI: Siderophile elements in ordinary chondrites. *Geochimica et Cosmochimica Acta* 50:2815–2832.

Sears D. W., Grossman J. N., Ross L. M., and Mills A. A. 1980. Measuring metamorphic history of unequilibrated ordinary chondrites. *Nature* 287:791–795.

Sears D. W. G., Grossman J. N., and Melcher C. L. 1982. Chemical and physical studies of type 3 c chondrites 1: Metamorphism related studies of Antarctic and other type 3 ordinary chondrites. *Geochimica et Cosmochimica Acta* 46:2471–2481.

Slater-Reynolds V. and McSween H. Y. Jr.. 2005. Peak metamorphic temperatures in type 6 ordinary chondrites:

An evaluation of pyroxene and plagioclase goethermometry. *Meteoritics & Planetary Science* 40:745–754.

Smith B. A. and Goldstein J. I. 1977. The metallic microstructures and thermal histories of severely reheated chondrites. *Geochimica et Cosmochimica Acta* 41:1061–1072.

Van Schmus W. R. and Wood J. A. 1967. A chemical-petrologic classification for the chondrite meteorites. *Geochimica et Cosmochimica Acta* 31:747–765.

Wasson J. T. 2000. Oxygen-isotopic evolution in the solar nebula. *Reviews of Geophysics* 38:491–512.

Wasson J. T. and Trigo-Rodríguez J. M. 2004. Evaporation during chondrule formation, recondensation as fine particles and the condensation of S and other volatile elements (abstract #2140). 35th Lunar and Planetary Science Conference. CD-ROM.